Introduction to a many-body description of semiconductor lasers

Weng Chow, Sandia National Labs

Outline

1) Past: Free-carrier theory
2) Present: Many-body description
3) Evolving: Quantum-dot gain theory

Collaborations

Stephan Koch (Philipps University), Peter Smowton and Peter Blood (Cardiff University), Michael Lorke and Frank Jahnke (Bremen University), Stephan Michael and Christian Schneider (Kaiserslautern University), Andreas Knorr (Technical University, Berlin)

Thanks to:

Sandia Laboratory Research and Development (LDRD) program

Humboldt Foundation

Review of semiconductor laser gain

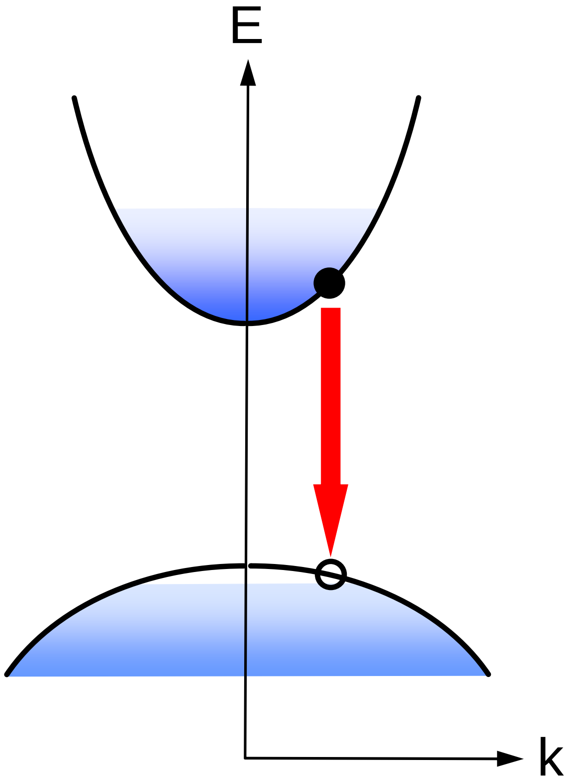

Gain spectrum

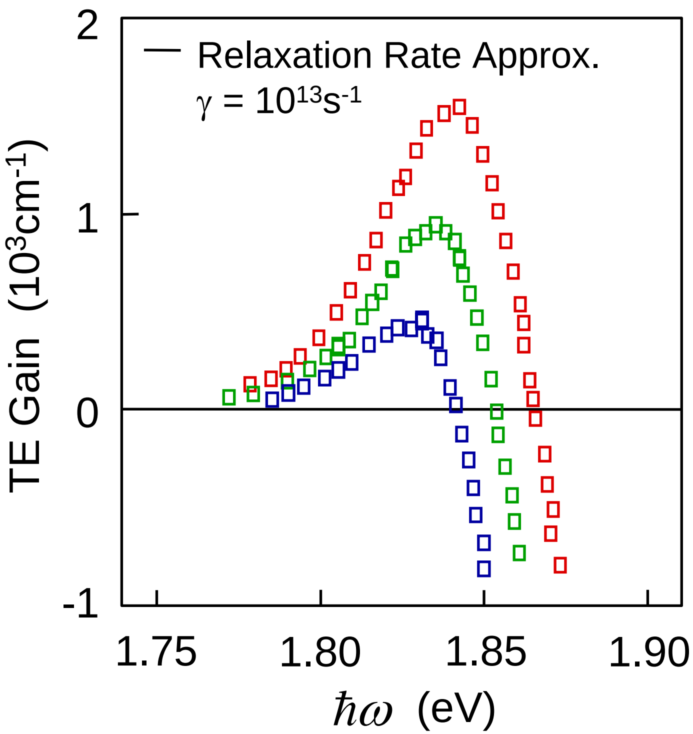

6.8nm $Ga_{0.41}In_{0.59}P$ / $(Al_{0.5}Ga_{0.5})_{0.51}In_{0.49}P$

Expt. data from P.M. Smowton and P. Blood, Cardiff University

Review of semiconductor laser gain

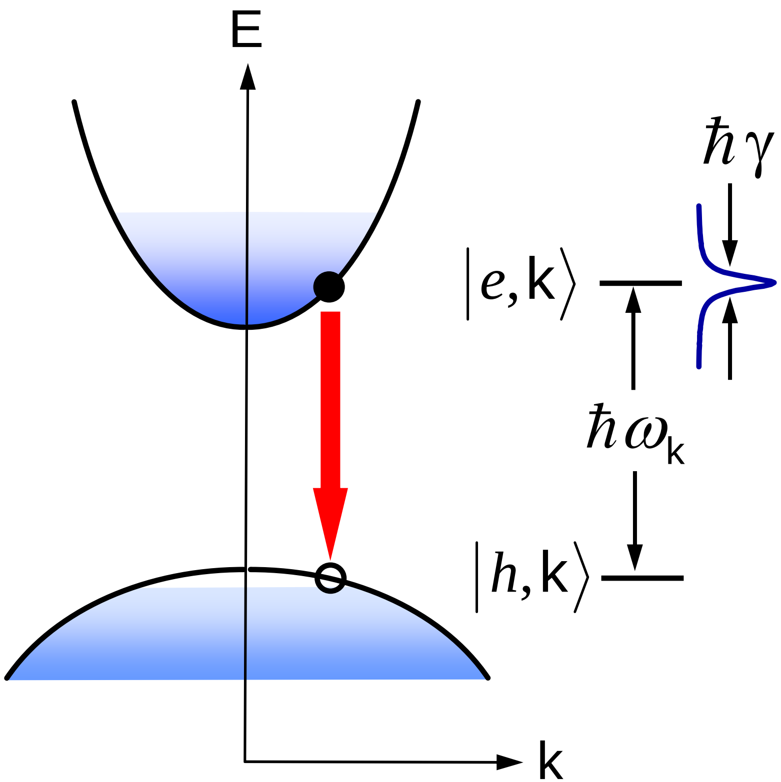

Gain spectrum

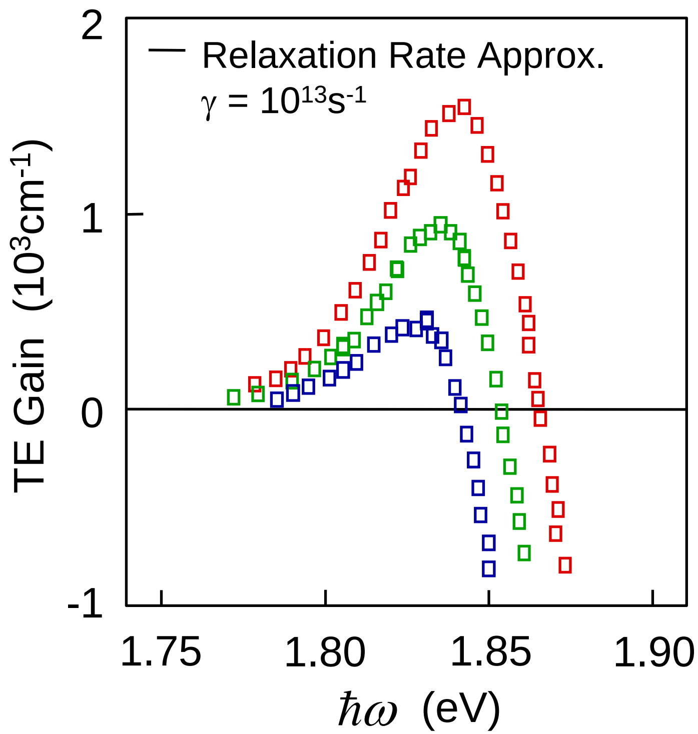

6.8nm $Ga_{0.41}In_{0.59}P$ / $(Al_{0.5}Ga_{0.5})_{0.51}In_{0.49}P$

Expt. data from P.M. Smowton and P. Blood, Cardiff University

Free-carrier description

$$\text{Gain}: \quad G \propto \sum_k |\underbrace{\mu_k}_{\text{Dipole matrix element}}|^2 \underbrace{[n_{ek} + n_{hk} - 1]}_{\text{Population inversion}} \underbrace{L(\omega_k - \nu)}_{\text{Lineshape function (collision effects)}}$$

Dipole matrix element

Population inversion

Lineshape function (collision effects)

Review of semiconductor laser gain

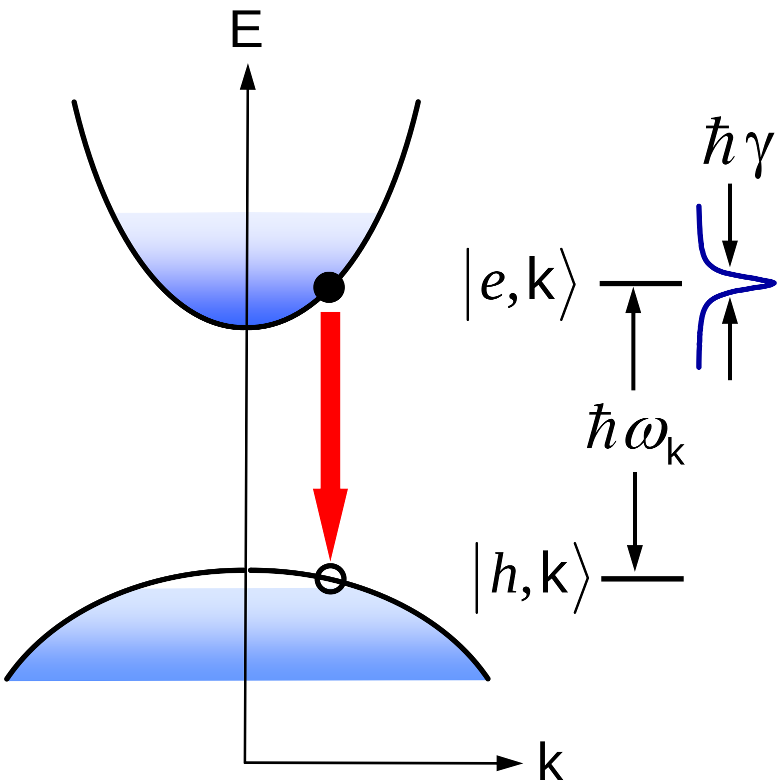

Gain spectrum

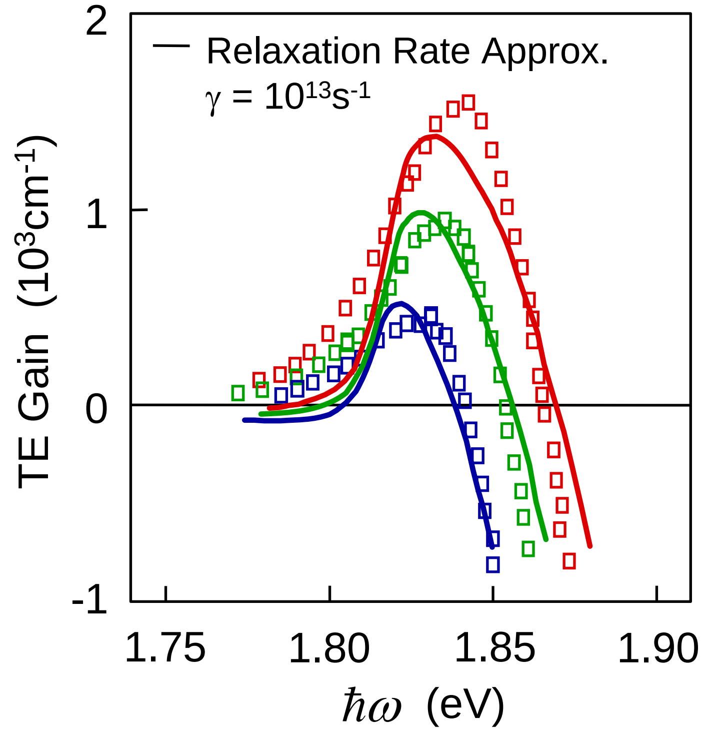

6.8nm $Ga_{0.41}In_{0.59}P$ / $(Al_{0.5}Ga_{0.5})_{0.51}In_{0.49}P$

Expt. data from P.M. Smowton and P. Blood, Cardiff University

Free-carrier description

Gain : $$G \propto \sum_k |\mu_k|^2 \underbrace{\left[n_{ek} + n_{hk} - 1\right]}_{\text{Population inversion}} \underbrace{L(\omega_k - \nu)}_{\text{Lineshape function (collision effects)}}$$

Dipole matrix element

(1) Semiclassical laser theory

$$\frac{d\mathcal{E}}{dz} = g\mathcal{E} = -\frac{\nu}{2\epsilon_0 nc} Im\left(\sum_k \mu_k \langle b_{-k} a_k \rangle\right)$$

Gain

(2) Equation of motion (Heisenberg Picture)

$$\frac{dO}{dt} = \frac{i}{\hbar}\left[H, O\right]$$

(3) Hamiltonian

$$H = \sum_k \left(\varepsilon_{ek} a_k^\dagger a_k + \varepsilon_{hk} b_{-k}^\dagger b_{-k}\right)$$ **Kinetic energy**

$$-\sum_k \left(\mu_k a_k^\dagger b_{-k}^\dagger + \mu_k^* b_{-k} a_k\right) E\left(z,t\right)$$ **Light-matter interaction**

$$+\frac{1}{2}\sum_{k,k',q} V_q \left(a_{k+q}^\dagger a_{k'-q}^\dagger a_{k'} a_k + b_{k+q}^\dagger b_{k'-q}^\dagger b_{k'} b_k - 2a_{k+q}^\dagger b_{k'-q}^\dagger b_{k'} a_k\right)$$

Coulomb interaction

(4) Anticommutation relations

$$\left\{a_k, a_{k'}^\dagger\right\} = \left\{b_k, b_{k'}^\dagger\right\} = \delta_{k,k'} \qquad \{a_k, a_{k'}\} = \{b_k, b_{k'}\} = 0$$

Quantum statistics: Identical particles

1) Symmetry (or antisymmetry) of wavefunctions

$$\psi\left(r_1, r_2\right) = c_1 \phi_a\left(r_1\right) \phi_b\left(r_2\right) - c_2 \phi_b\left(r_1\right) \phi_a\left(r_2\right)$$

2) Bookkeeping $\longrightarrow$ Second quantization

Anticommutation relations

$$\left\{a_k, a_{k'}^\dagger\right\} = \left\{b_k, b_{k'}^\dagger\right\} = \delta_{k,k'}$$

$$\left\{a_k, a_{k'}\right\} = \left\{b_k, b_{k'}\right\} = 0$$

$$\boxed{\{A, B\} = AB + BA}$$

3) Quantum statistics and Coulomb interaction

$$\frac{e^2}{4\pi\varepsilon_B r}$$

determines effective separation

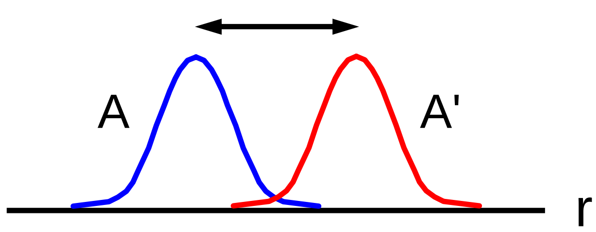

Problem

$$\frac{db_{-k}a_k}{dt} = -i\omega'_k p_k - \frac{i}{\hbar}\mu_k E(z,t)\left[a_k^\dagger a_k + b_{-k}^\dagger b_{-k} - 1\right] + \frac{i}{\hbar}\sum_{k',q\neq 0} V_q \left[... - \ a_{k'+q}^\dagger b_{-k+q} a_{k'} a_k + ... \right]$$

Fix Factorization into products of $\begin{cases} p_k = \langle b_{-k}a_k \rangle \\ n_{ek} = \langle a_k^\dagger a_k \rangle \\ n_{hk} = \langle b_{-k}^\dagger b_{-k} \rangle \end{cases}$

Many-body Hamiltonian

→ $\frac{d}{dt}\langle AB \rangle_{HF}$ Bandgap renormalization and Coulomb enhancement

→ $\frac{d}{dt}\langle \delta ABCD \rangle$ Screening and collisions

→ $\frac{d}{dt}\langle \delta ABCDEF \rangle$

$\vdots$

Polarization equation of motion

$$\omega_k^{(0)} - \sum_{\mathbf{k}'} V_{kk'}\left(n_{ek'} + n_{hk'}\right) \qquad\qquad \frac{2\mu_k E}{\hbar} + \sum_{k'} V_{kk'} p_{k'}$$

$$\frac{dp_k}{dt} = -i\omega_k p_k - i\Omega_k \left(n_{ek} + n_{hk} - 1\right)$$

$$+S_k^{c-c} + S_k^{c-p}$$

Polarization equation of motion

$$\omega_k^{(0)} - \sum_{\mathbf{k}'} V_{kk'}\left(n_{ek'} + n_{hk'}\right) \qquad \frac{2\mu_k E}{\hbar} + \sum_{k'} V_{kk'} p_{k'}$$

$$\frac{dp_k}{dt} = -i\omega_k p_k - i\Omega_k \left(n_{ek} + n_{hk} - 1\right)$$

$$+ S_k^{c-c} + S_k^{c-p}$$

$$-\sigma_k^d p_k$$

Exponential decay

Typical

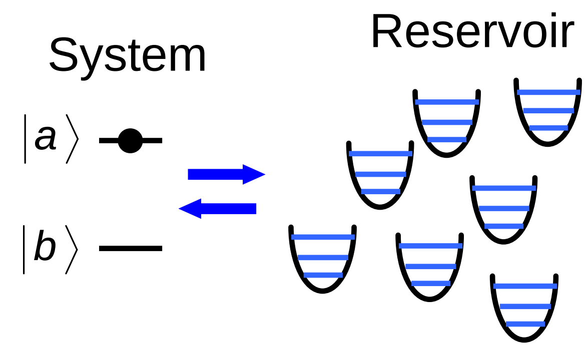

Polarization equation of motion

$$\omega_k^{(0)} - \sum_{\mathbf{k}'} V_{kk'}\left(n_{ek'} + n_{hk'}\right) \qquad \frac{2\mu_k E}{\hbar} + \sum_{k'} V_{kk'} p_{k'}$$

$$\frac{dp_k}{dt} = -i\omega_k p_k - i\Omega_k \left(n_{ek} + n_{hk} - 1\right)$$

$$+ S_k^{c-c} + S_k^{c-p}$$

$$-\sigma_k^d p_k + \sum_k \sigma_{k,k'}^{nd} p_{k'}$$

Diagonal **Nondiagonal**

System Reservoir

Typical

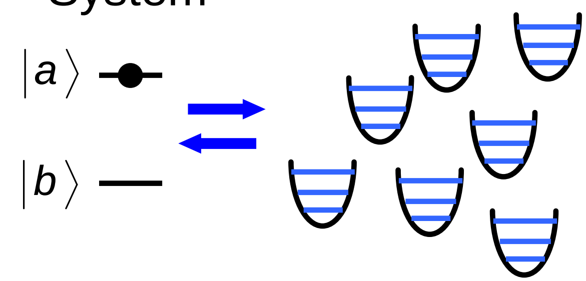

System Reservoir

Semiconductor

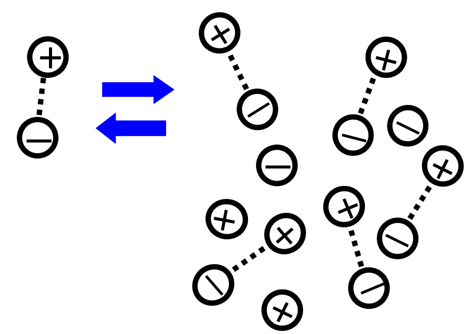

System is its own reservoir

Quantum well gain spectrum

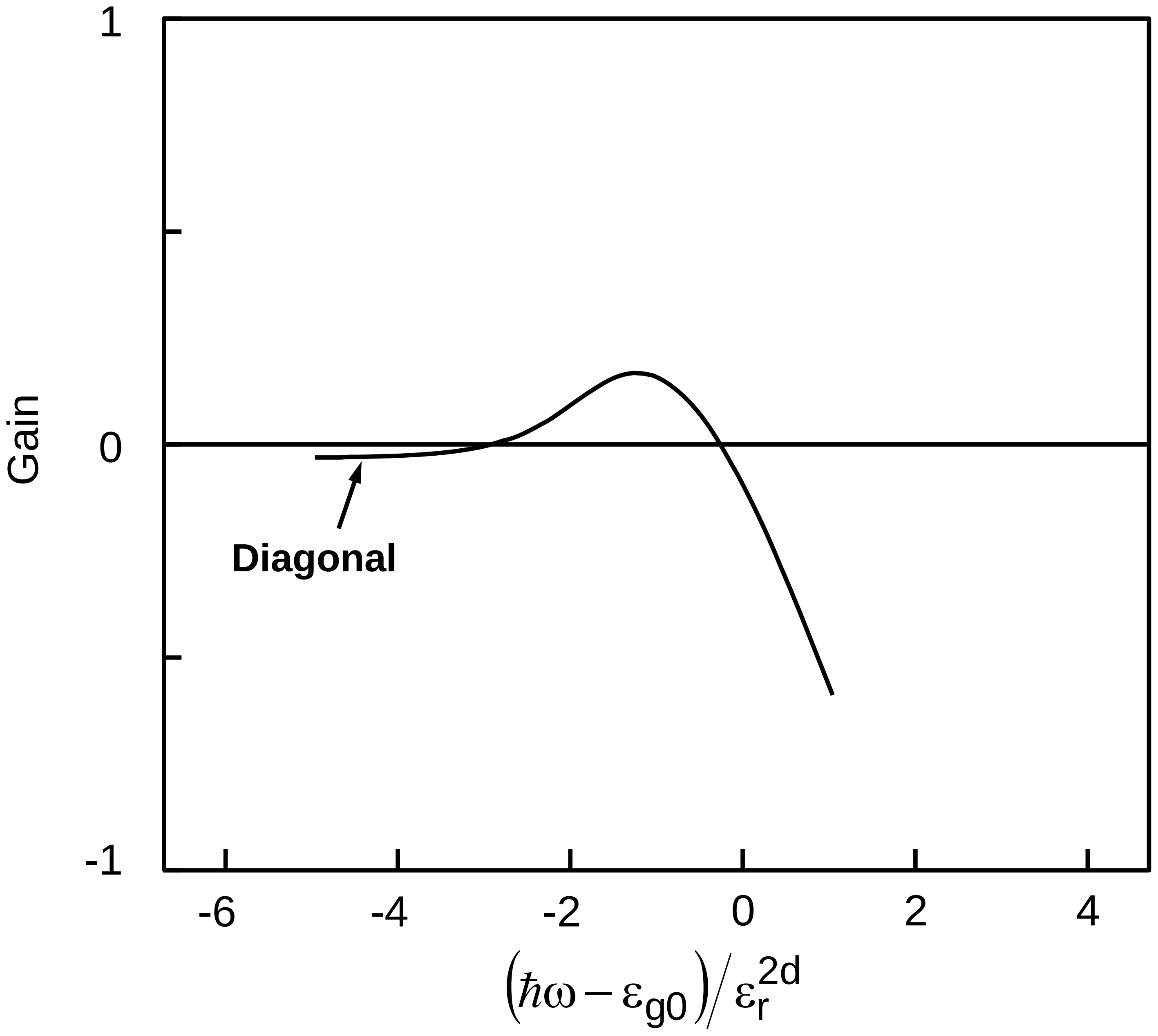

mbt\mbt9a

Quantum well gain spectrum

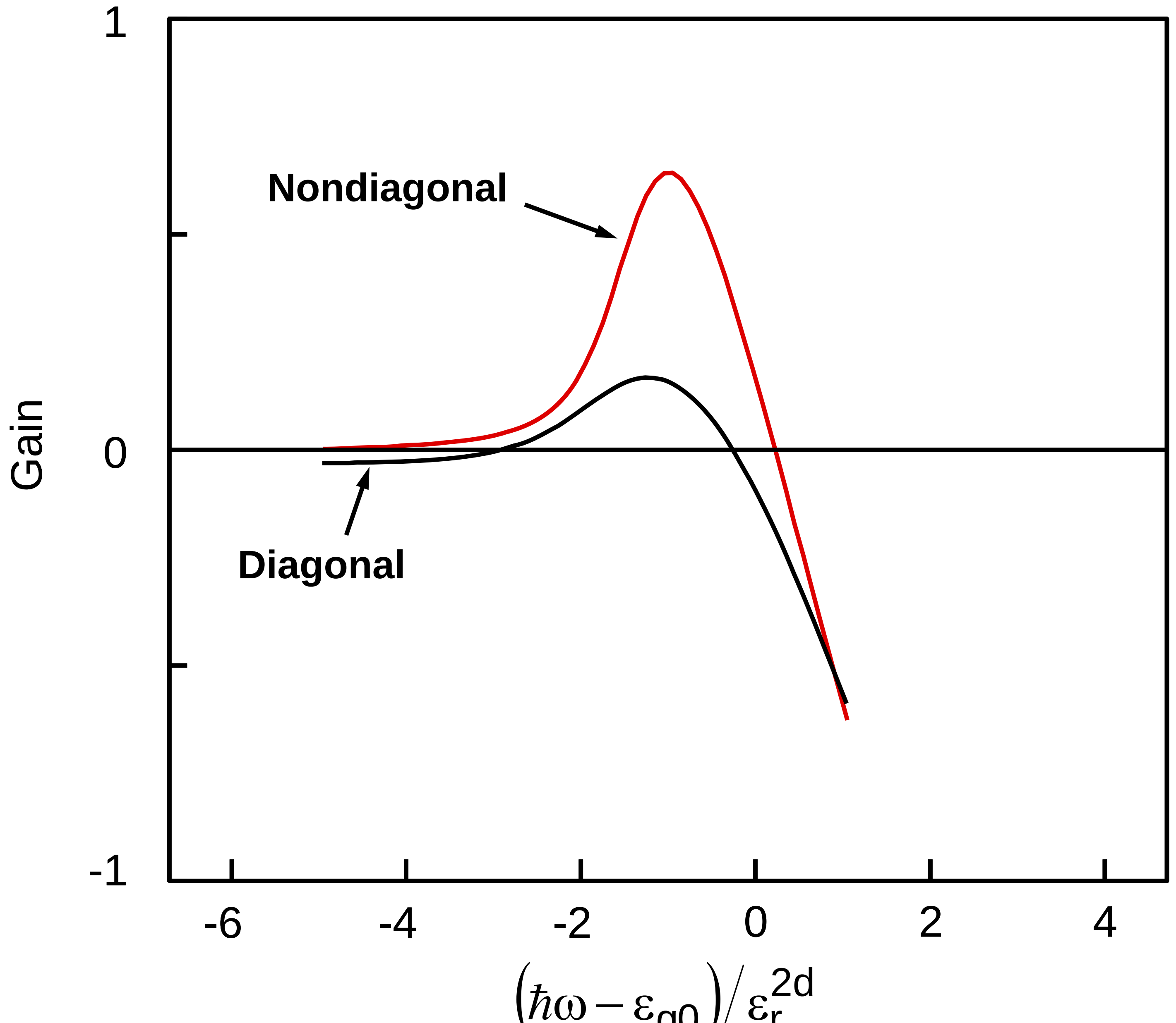

mbt\mbt9a

6.8 nm $Ga_{0.41}In_{0.59}P$ / $(Al_{0.5}Ga_{0.5})_{0.51}In_{0.49}P$

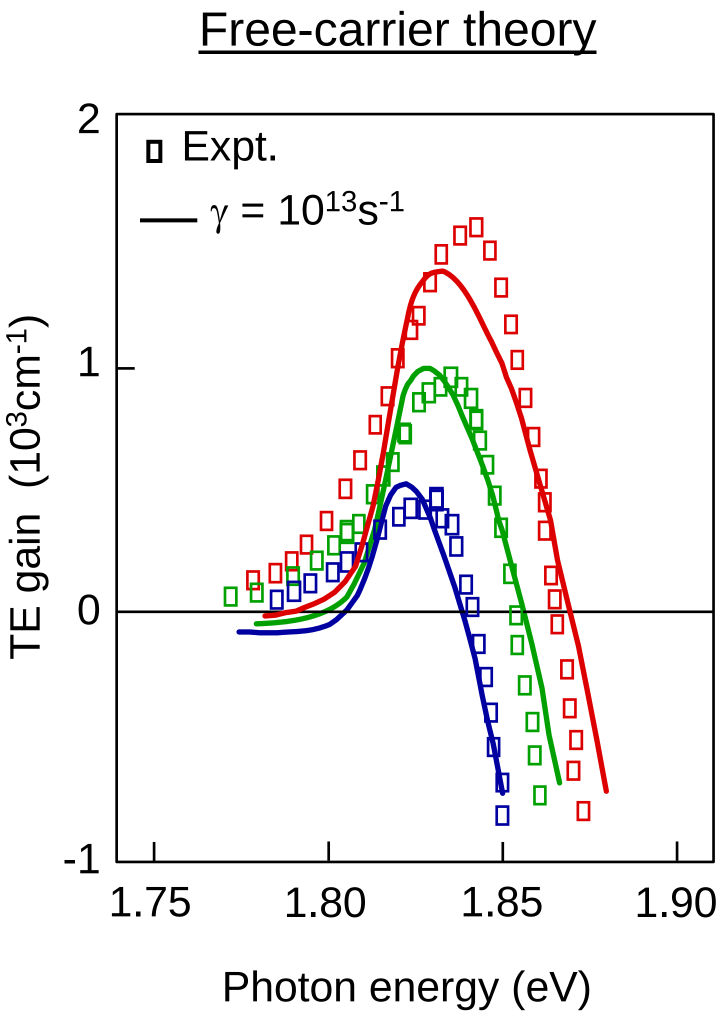

6.8 nm $Ga_{0.41}In_{0.59}P$ / $(Al_{0.5}Ga_{0.5})_{0.51}In_{0.49}P$

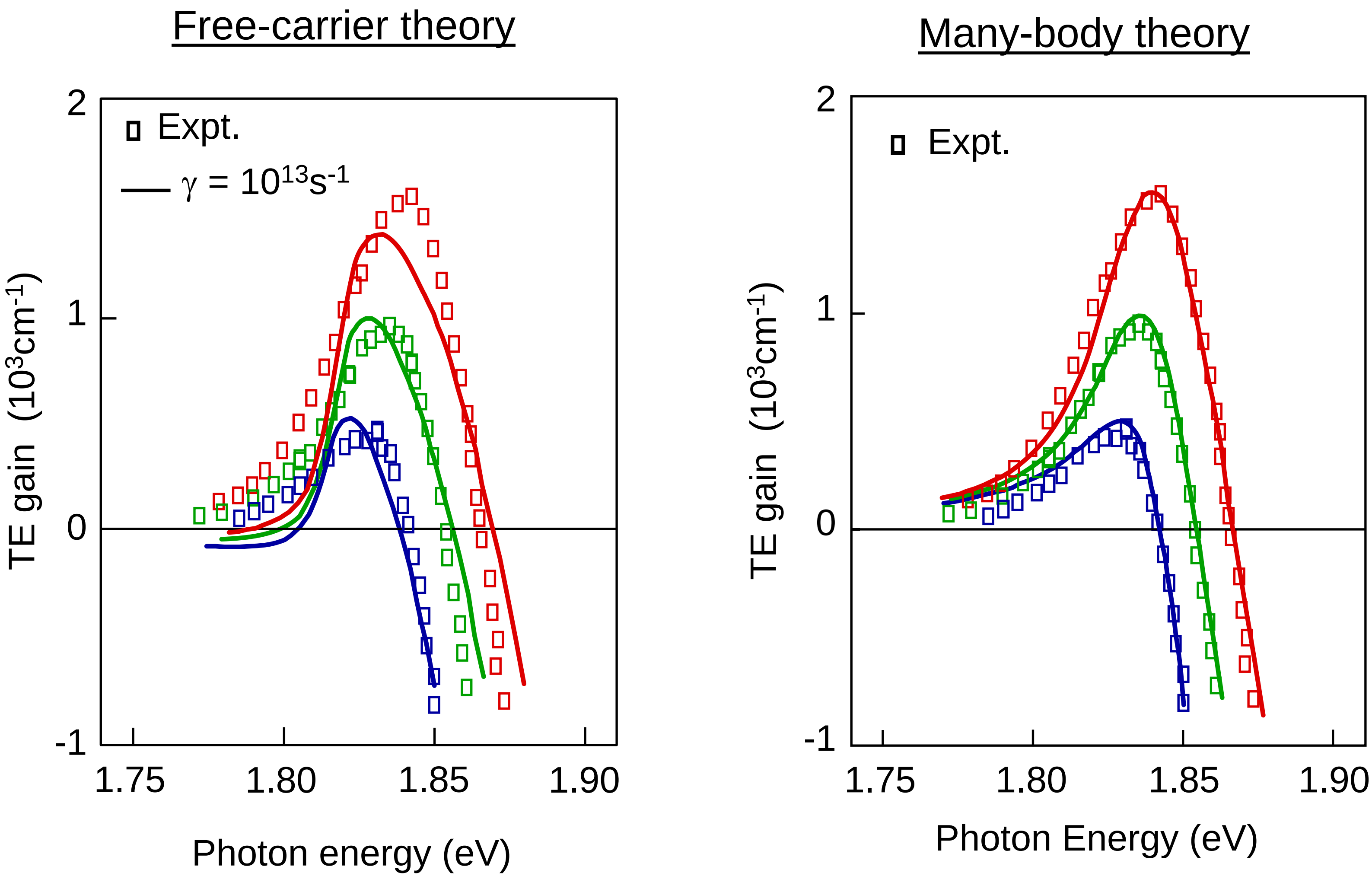

WWC, P. M. Smowton, P. Blood, A. Girdnt, F. Jahnke and S. W. Koch, APL.**71**, 157 (1997)

With many-body effects:

Fix absorption below bandgap

Eliminate dephasing rate as free parameter

Input: growth sheet and bandstructure parameters

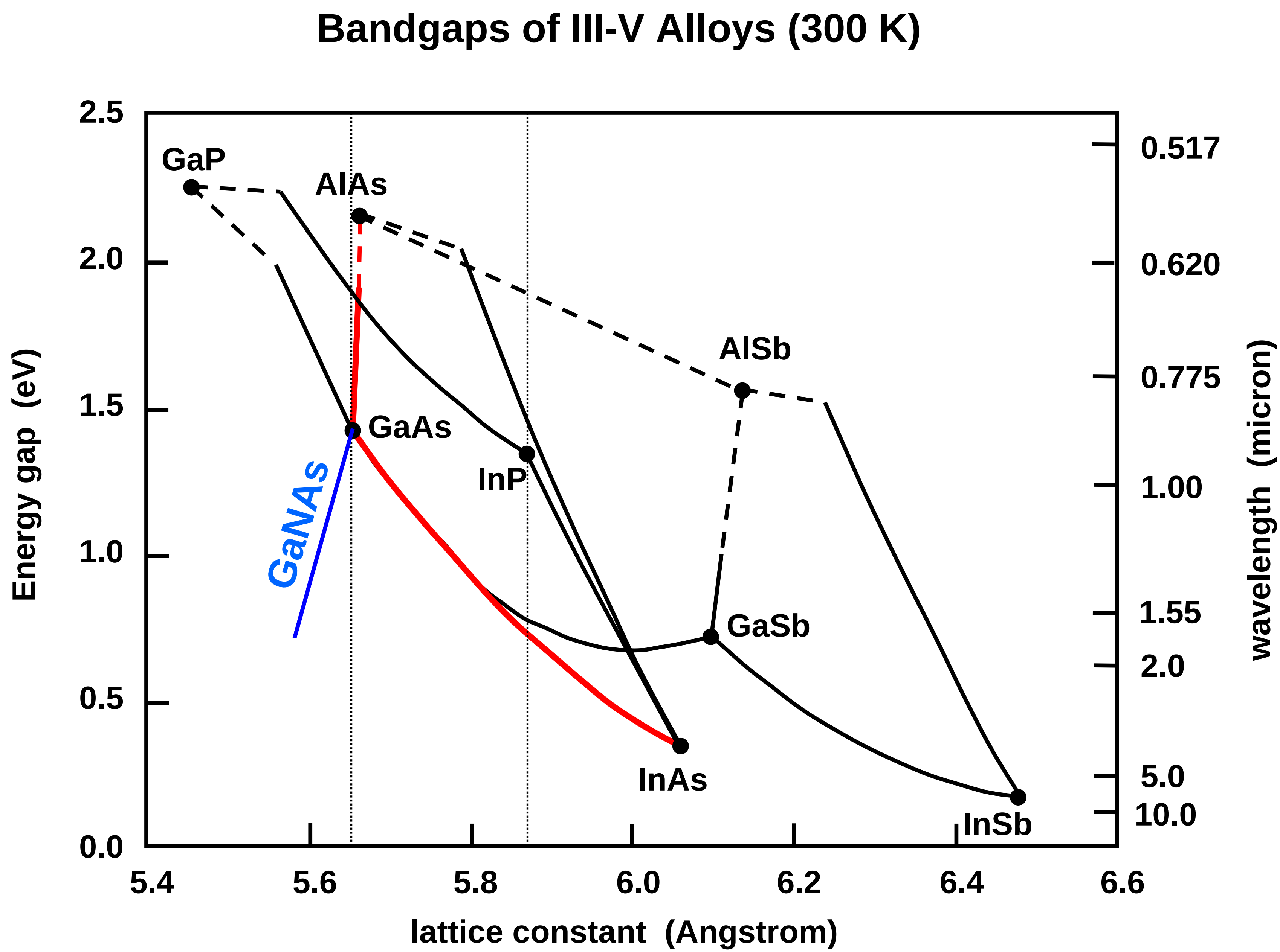

Bandgaps of III-V Alloys (300 K)
2.5
2.0
1.5
1.0
0.5
0.0
Energy gap (eV)
GaP
AlAs
AlSb
GaAs
InP
GaNAs
GaSb
InAs
InSb
0.517
0.620
0.775
1.00
1.55
2.0
5.0
10.0
wavelength (micron)
5.4
5.6
5.8
6.0
6.2
6.4
6.6
lattice constant (Angstrom)

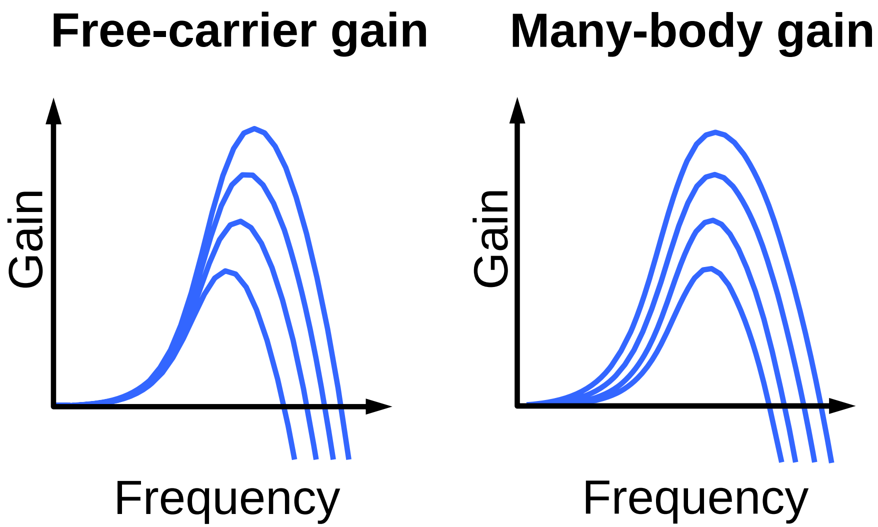
Free-carrier gain
Many-body gain
Gain
Frequency
Gain
Frequency

Free-carrier gain

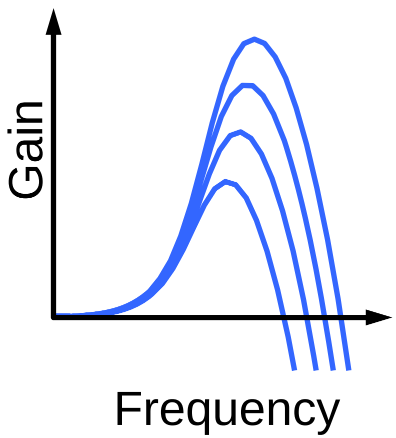

Many-body gain

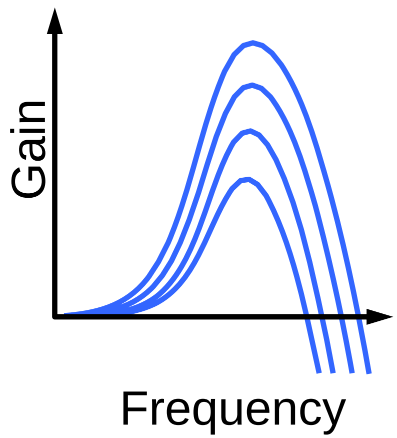

Vertical-Cavity Surface-Emitting Laser (VCSEL)

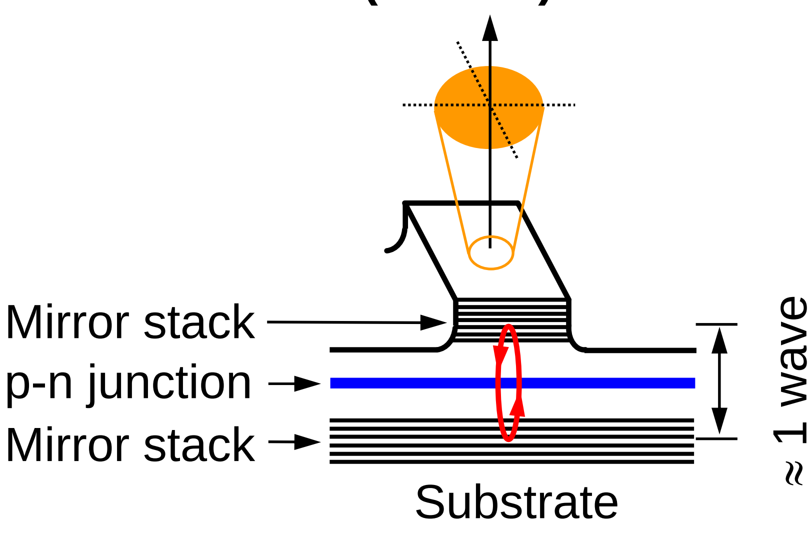

Temperature dependence of VCSEL threshold current

8nm $In_{0.2}Ga_{0.8}As$-GaAs VCSEL

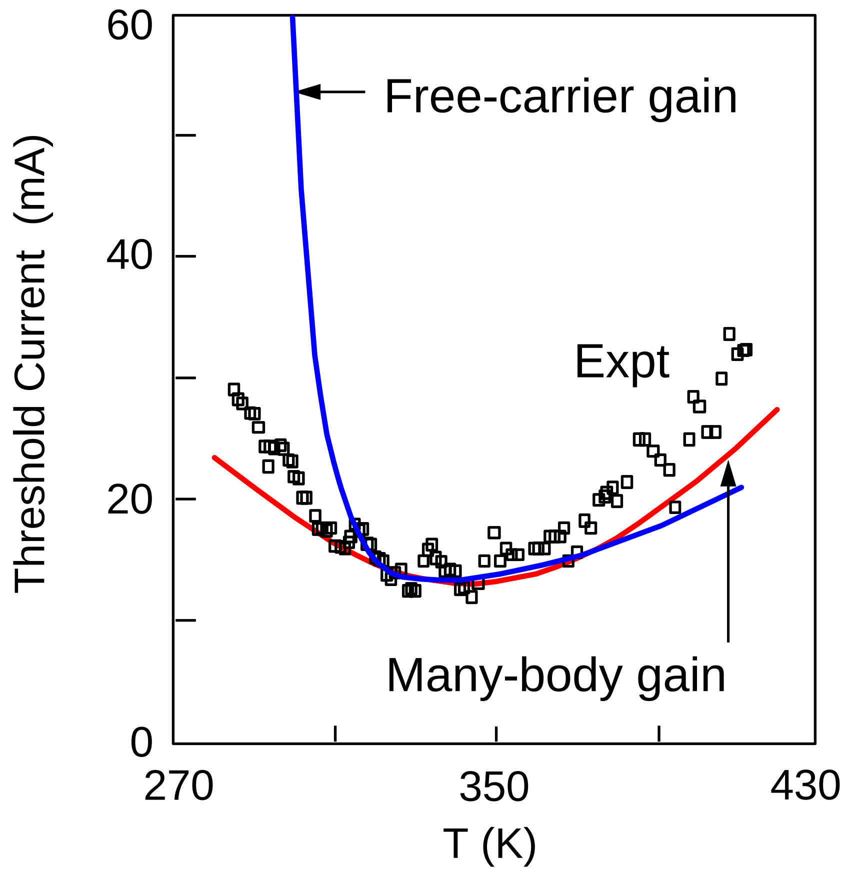

WWC, Corzine, Young, Coldren
APL 66, 2560 (1995)

Visible and ultraviolet lasers: wide bandgap Group-III Nitrides

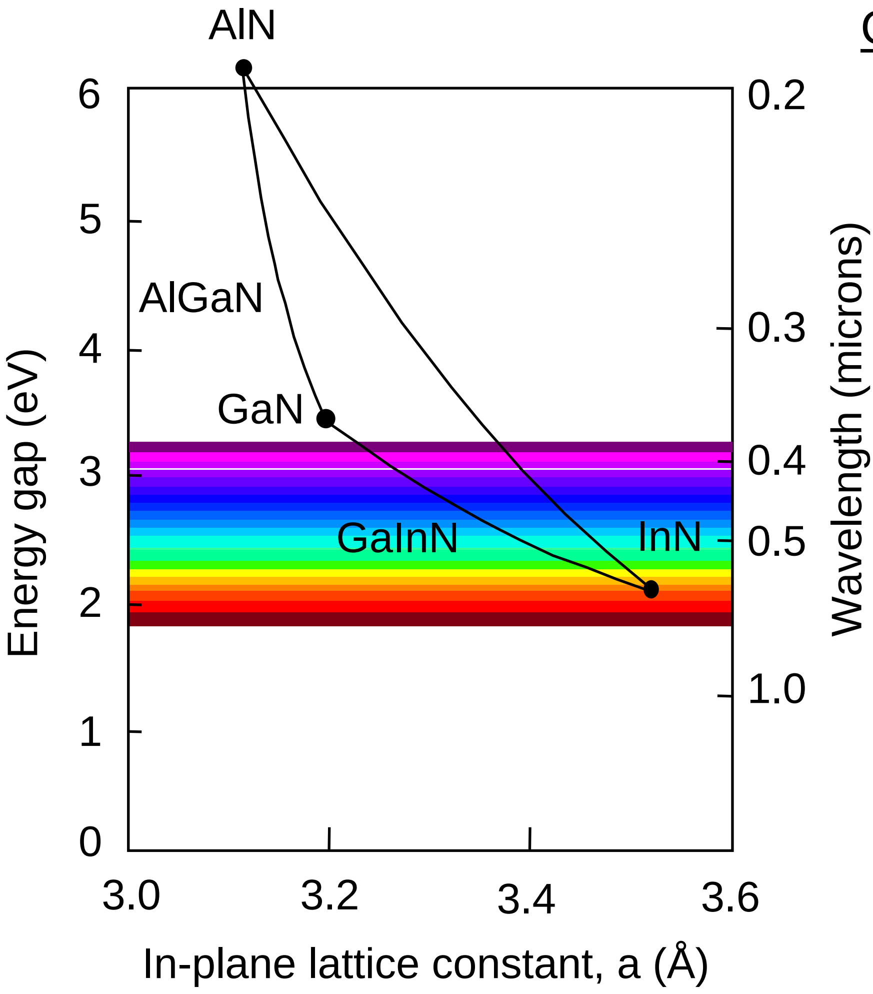

<u>Group-III nitride vs. conventional III-V lasers</u>

High exciton binding energy
(23meV for GaN vs. 5meV for GaAs)

→ **Strong many-body Coulomb effects**

Wurtzite crystal symmetry

→ **Strong quantum confined Stark effect**

Strong many-body and bandstructure effects in Wurtzite InGaN

Conventional diode laser

Strong many-body effects

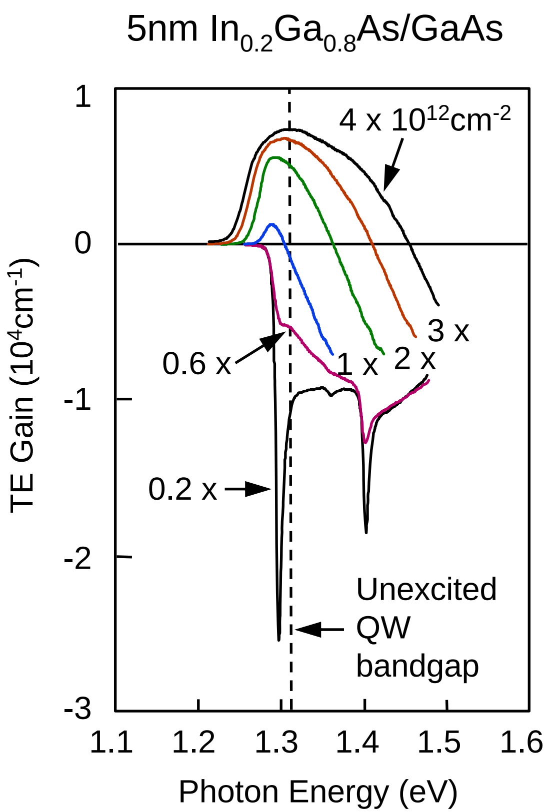

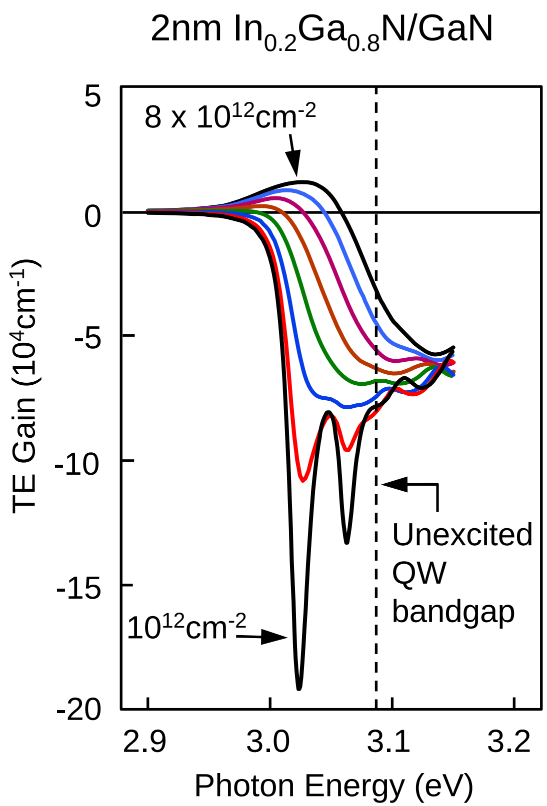

Strong many-body and bandstructure effects in Wurtzite InGaN

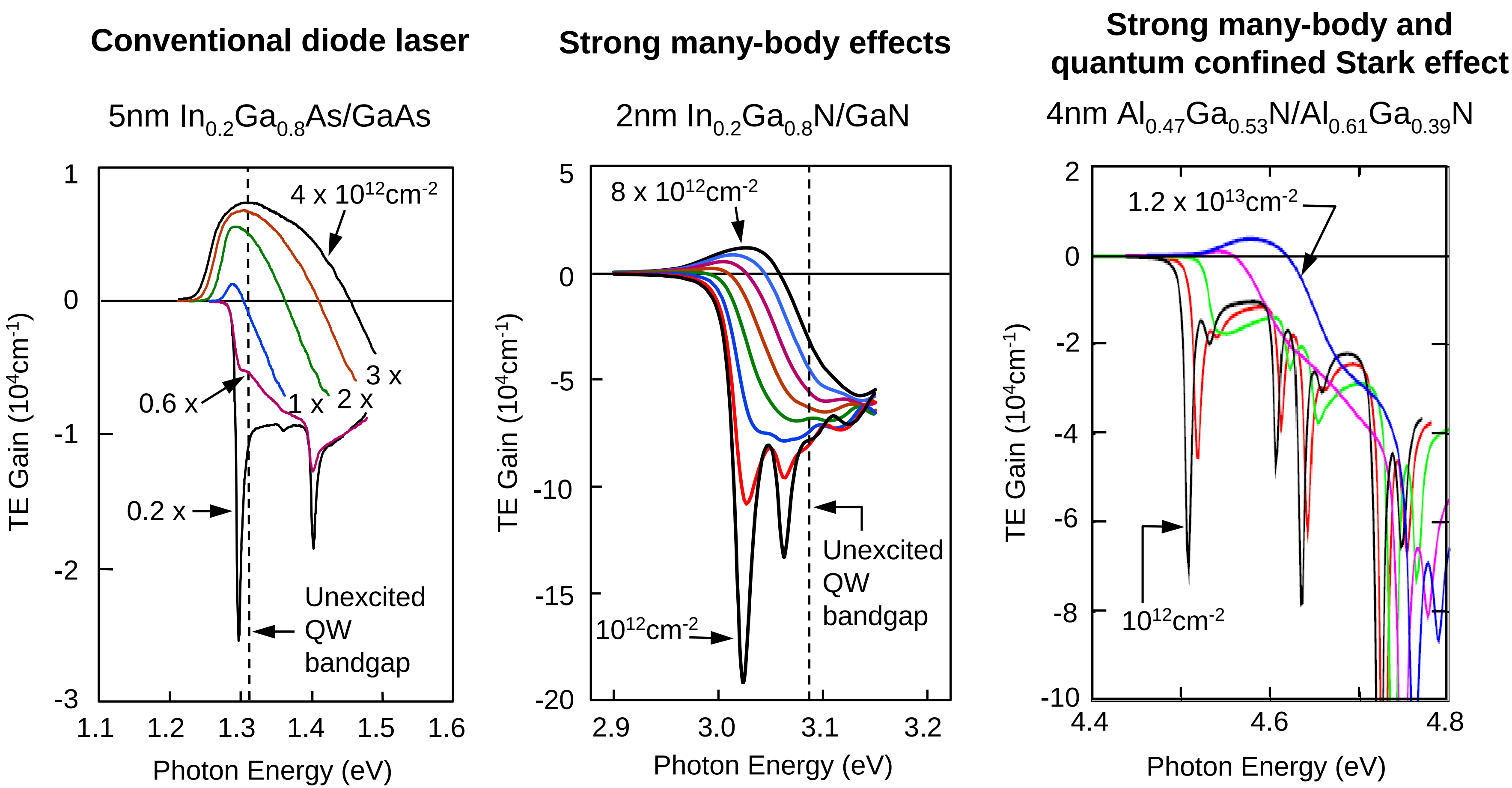

WWC and M. Kneissl (PARC)

J. Appl. Phys. **98**, 114502 (2005)

T. M. Al Tahtamouni, N. Nepal, J. Y. Lin, H. X. Jiang (KSU) and WWC, APL **89** 131922 (2006)

Uses of gain theory

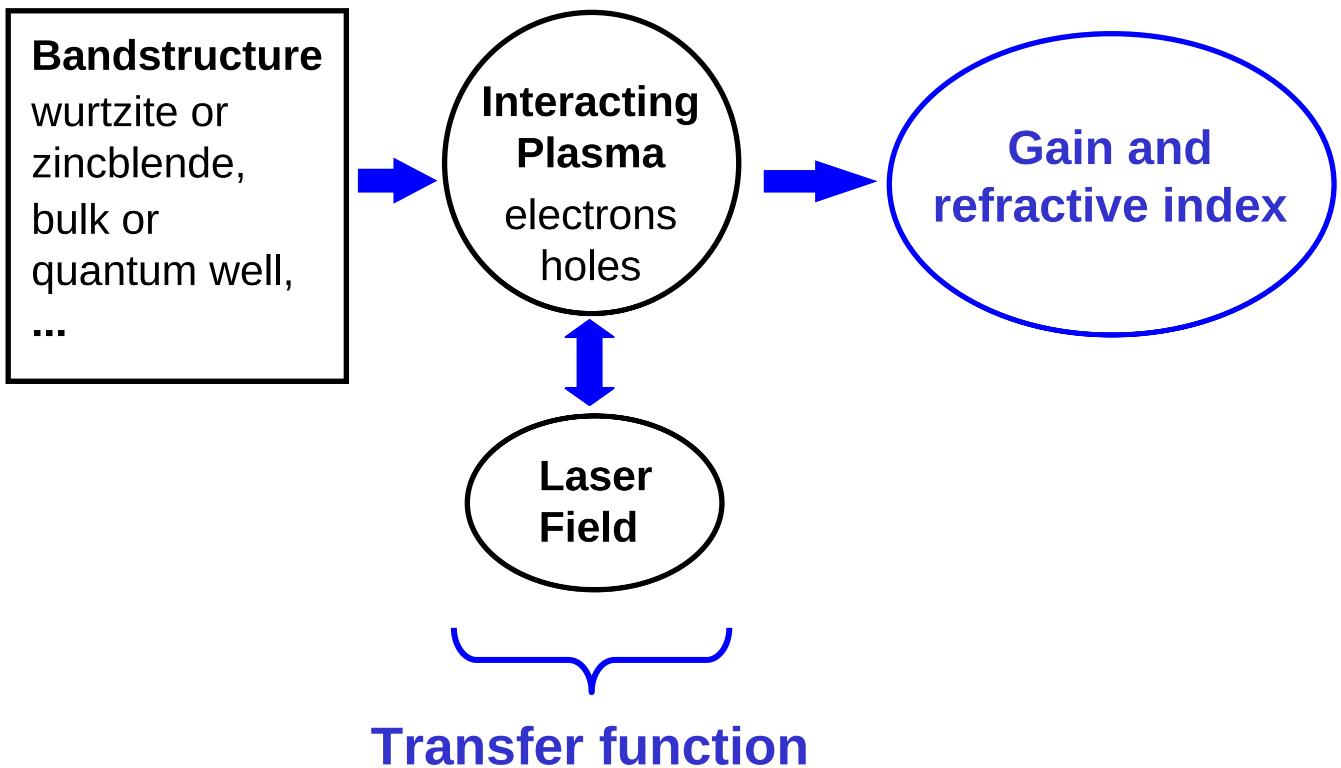

Bandstructure → **Gain properties**

Barrier Influence on Threshold Current Density in AlGaN Lasers

3nm $Al_{0.46}Ga_{0.54}N$ / $Al_yGa_{1-y}N$, 300K, 280 nm

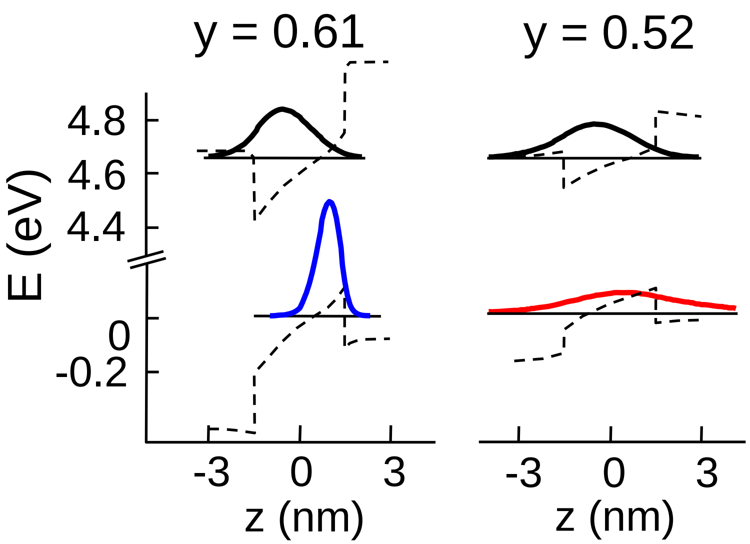

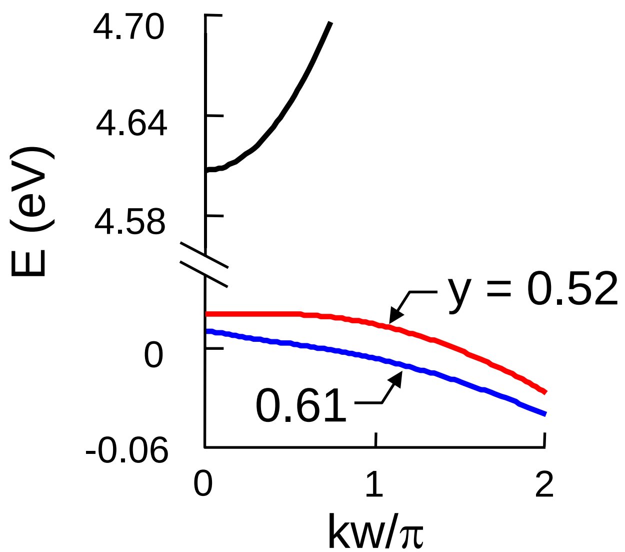

Barrier Influence on Threshold Current Density in AlGaN Lasers

3nm $Al_{0.46}Ga_{0.54}N$ / $Al_yGa_{1-y}N$, 300K, 280 nm

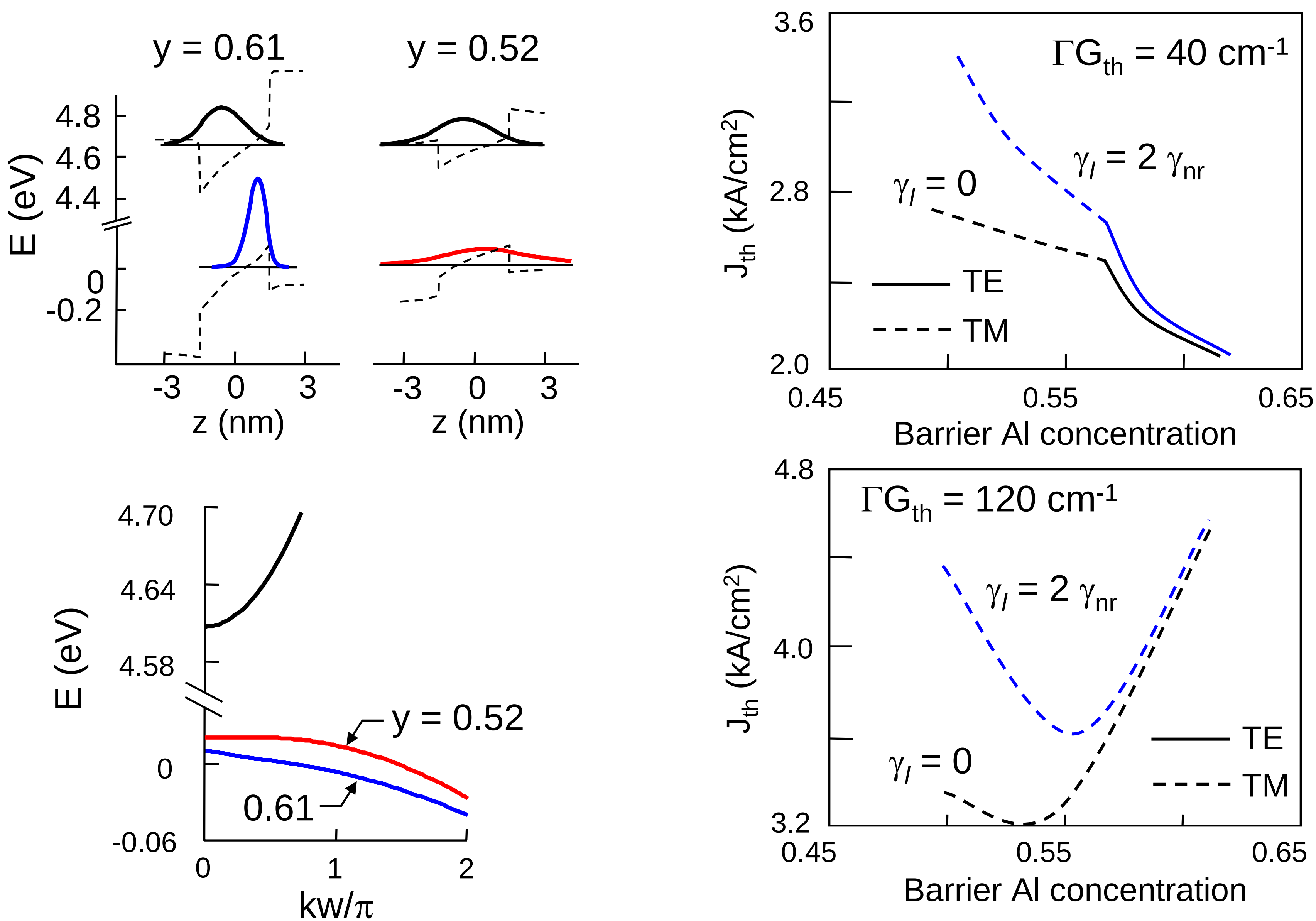

WWC, M. Kneissl, J.E. Northrup and N.M. Johnson, APL **90**, 101116 (2007)

Quantum well

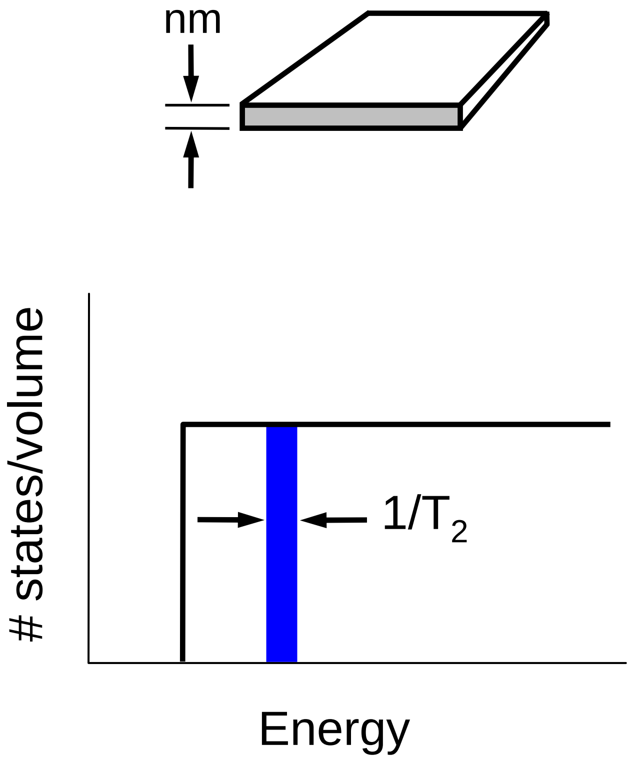

Quantum dot

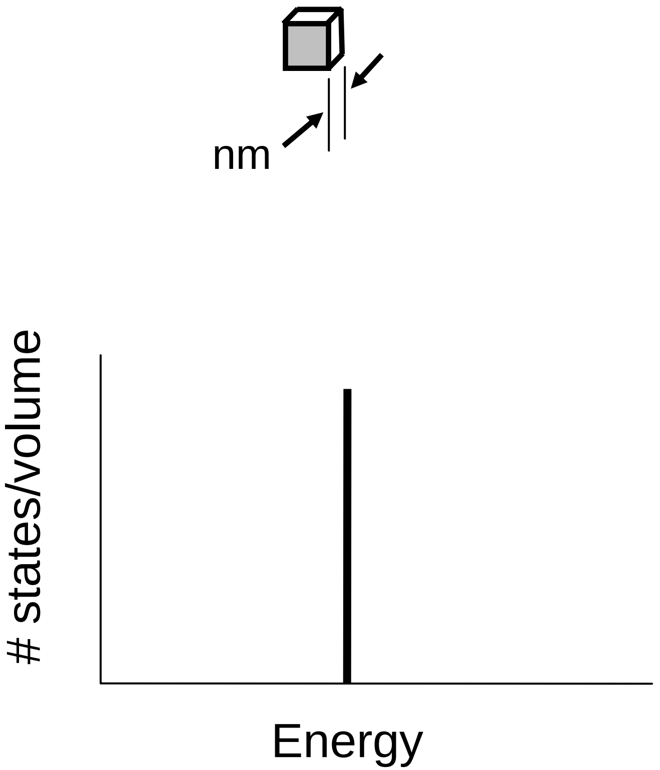

Quantum dot $\overset{?}{=}$ atom

Active region

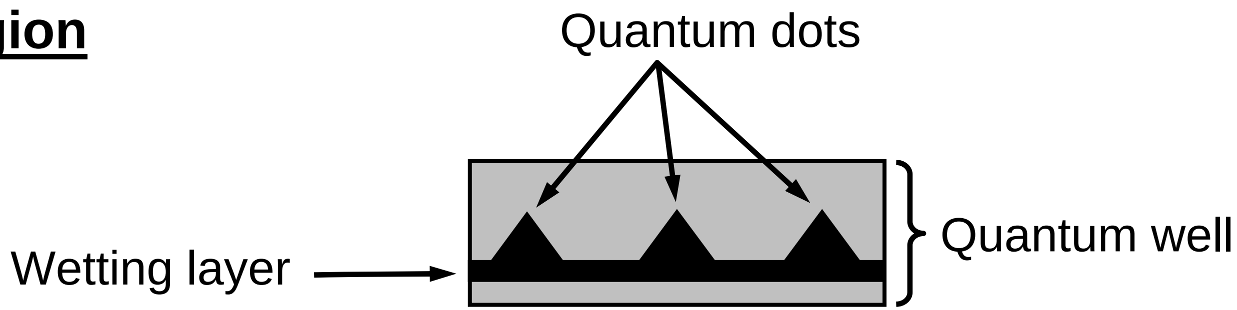

Dot-Well Hamiltonian

$$H = \sum_n \varepsilon_n a_n^\dagger a_n + \sum_m \varepsilon_m b_m^\dagger b_m$$

Single-particle

$$- \sum_{n,m} \left(\mu_{nm} a_n^\dagger b_m^\dagger + \mu_{nm}^* b_m a_n \right) E(z,t)$$

Light-matter interaction

$$+ \frac{1}{2} \sum_{n,m,r,s} W_{nm}^{rs} a_r^\dagger a_s^\dagger a_m a_n + \frac{1}{2} \sum_{n,m,r,s} W_{nm}^{rs} b_r^\dagger b_s^\dagger b_m b_n - \sum_{n,m,r,s} W_{nm}^{rs} a_r^\dagger b_s^\dagger b_m a_n$$

$$+ \sum_{n,q} \hbar G_q a_{n+q}^\dagger a_n \left(b_q + b_{-q}^\dagger \right)$$

Carrier - phonon

Carrier - carrier

Coulomb matrix element

$$W_{nk}^{rk'} = \int d^3r \, d^3r' \, \phi_r^* (\mathbf{r}) \, \phi_{k'}^* (\mathbf{r}') \, \frac{e^2}{4\pi\varepsilon_b \left| \mathbf{r} - \mathbf{r}' \right|} \phi_k (\mathbf{r}') \, \phi_n (\mathbf{r})$$

Complications with quantum dots

$$\frac{dp_\alpha}{dt} = -i\omega_\alpha p_\alpha - i\Omega_\alpha \left(n_{e\alpha} + n_{h\alpha} - 1\right)$$

$$+S_\alpha^{c-c} \; +S_\alpha^{c-p}$$

Carrier-carrier scattering

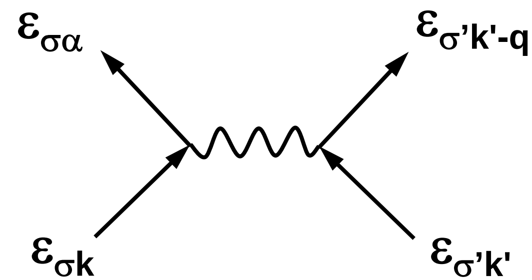

(diagonal contribution)

$$-p_\alpha \frac{2}{\hbar} \sum_{\mathbf{k}'} \sum_{\mathbf{q}} \sum_{\sigma} \sum_{\sigma'} \sum_{\mathbf{k}} \xi_{\alpha k} \left[{W_q}^2 - \frac{\delta_{\sigma,\sigma'}}{2} W_q W_{|\mathbf{k}'-\mathbf{q}-\mathbf{k}|} \right] \frac{1}{\Delta - i\delta\varepsilon}$$
$$\times \left[n_{|\mathbf{k}'-\mathbf{q}|\sigma'} \left(1 - n_{k'\sigma'}\right) \left(1 - n_{k\sigma}\right) + \left(1 - n_{|\mathbf{k}'-\mathbf{q}|\sigma'}\right) n_{k'\sigma'} n_{k\sigma} \right]$$

$$\delta\varepsilon = \hbar\omega - \underbrace{\varepsilon_{\overline{\sigma}\alpha} - \varepsilon_{\sigma k} + \varepsilon_{\sigma' k' - q} - \varepsilon_{\sigma' k'}}_{\text{Renormalized energies}}$$

Also, memory effects

Schneider, WWC and Koch, Phys. Rev. B 70, 235308, 2004.

Complications with quantum dots

$$\frac{dp_\alpha}{dt} = -i\omega_\alpha p_\alpha - i\Omega_\alpha \left(n_{e\alpha} + n_{h\alpha} - 1\right)$$

$$+S_\alpha^{c-c} \; +S_\alpha^{c-p}$$

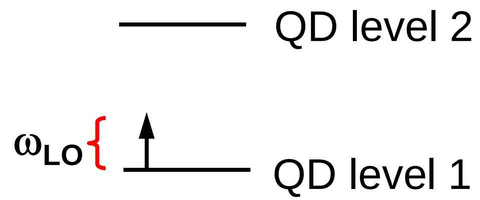

Carrier-phonon scattering

Complications with quantum dots

$$\frac{dp_\alpha}{dt} = -i\omega_\alpha p_\alpha - i\Omega_\alpha \left(n_{e\alpha} + n_{h\alpha} - 1\right)$$

$$+S_\alpha^{c-c} \; +S_\alpha^{c-p}$$

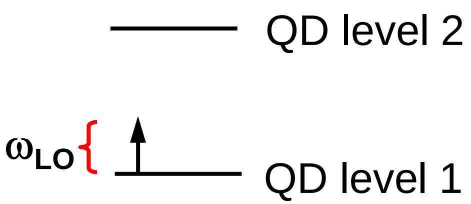

Carrier-phonon scattering

Nonperturbative treatment

$$-p_\alpha \int_0^\infty dt' \sum_{\mathbf{k}} \left| \frac{M_{\alpha k}}{\hbar} \right|^2 \sum_{\sigma=e,h} G_{k_\sigma}(t')\, G_{\alpha_\sigma}(t')\, e^{i(\varepsilon_{\alpha\sigma}-\varepsilon_{k\sigma})t'/\hbar}$$

$$\times \left\{ (1-n_{k\sigma}) \left[n_{LO} e^{i\omega_{LO}t'} + (n_{LO}+1)\, e^{-i\omega_{LO}t'} \right] + n_{k\sigma} \left[(n_{LO}+1)\, e^{i\omega_{LO}t'} + n_{LO} e^{-i\omega_{LO}t'} \right] \right\}$$

(diagonal contribution)

$$\frac{dG_{\alpha_\sigma}(t)}{dt} = -\int_0^t dt' \left[(n_{LO}+1)\, e^{-i\omega_{LO}t'} + n_{LO} e^{i\omega_{LO}t'} \right]$$

$$\times G_{\alpha_\sigma}(t-t') \sum_{\beta_{\sigma'}} \frac{\left| M_{\alpha_\sigma,\beta_{\sigma'}} \right|^2}{\hbar^2} G_{\beta_{\sigma'}}(t') \; \exp\left[i \frac{\varepsilon_{\alpha_\sigma} - \varepsilon_{\beta_{\sigma'}}}{\hbar} t' \right]$$

Inoshita, Sakaki, PRB 56,4355, 1997; Seebeck et al, PRB 71,125327, 2005

Inhomogeneous broadening

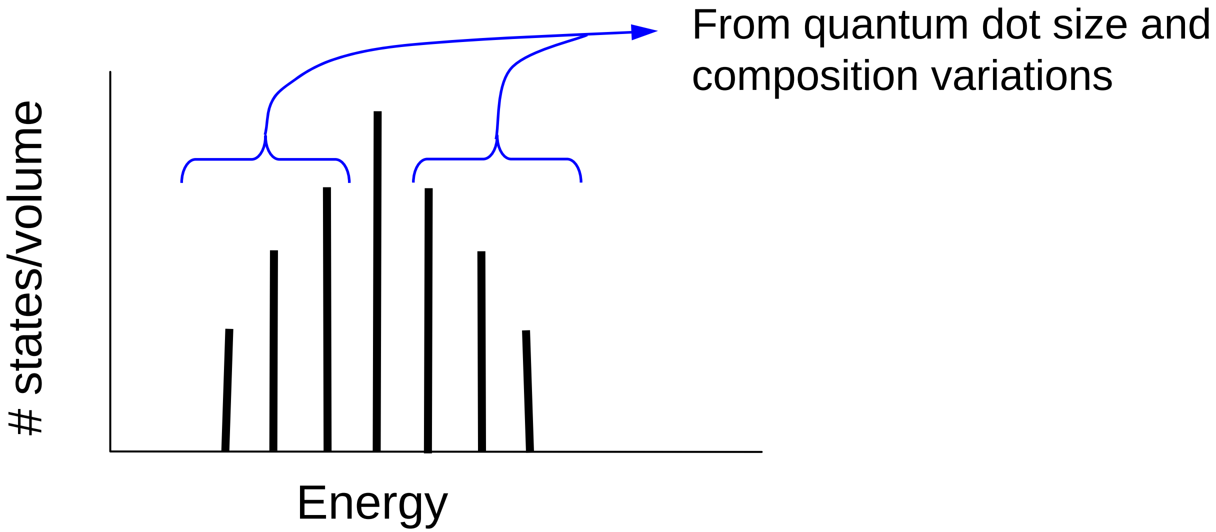

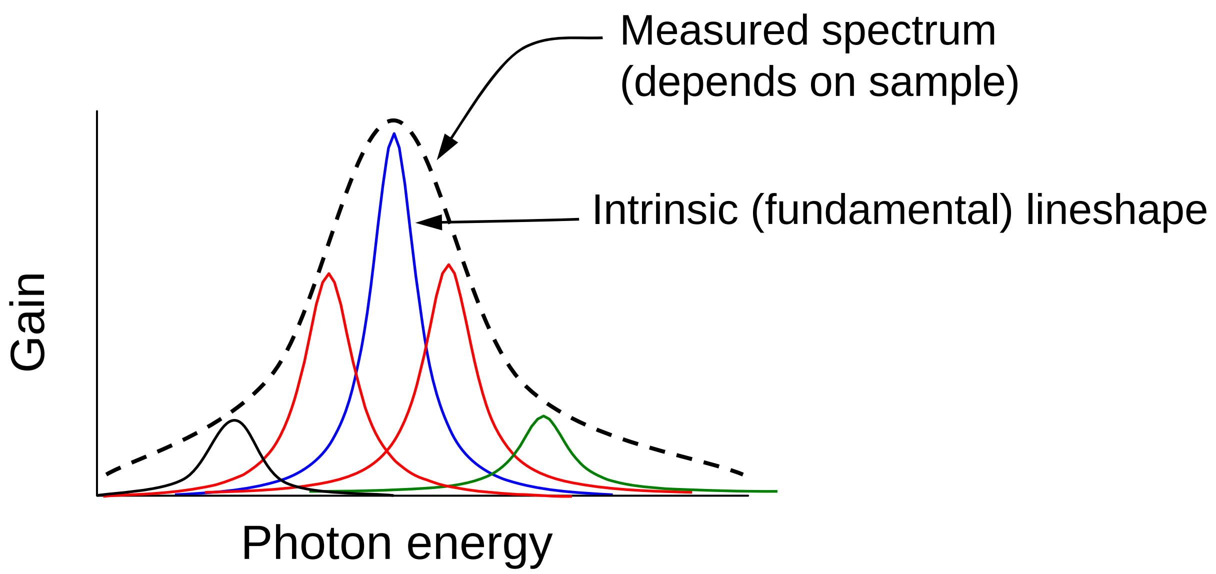

Homogeneously (intrinsically) broadened quantum-dot absorption and gain

InGaAs QD, N_D=5x10^{10}cm^{-2}, T=300K

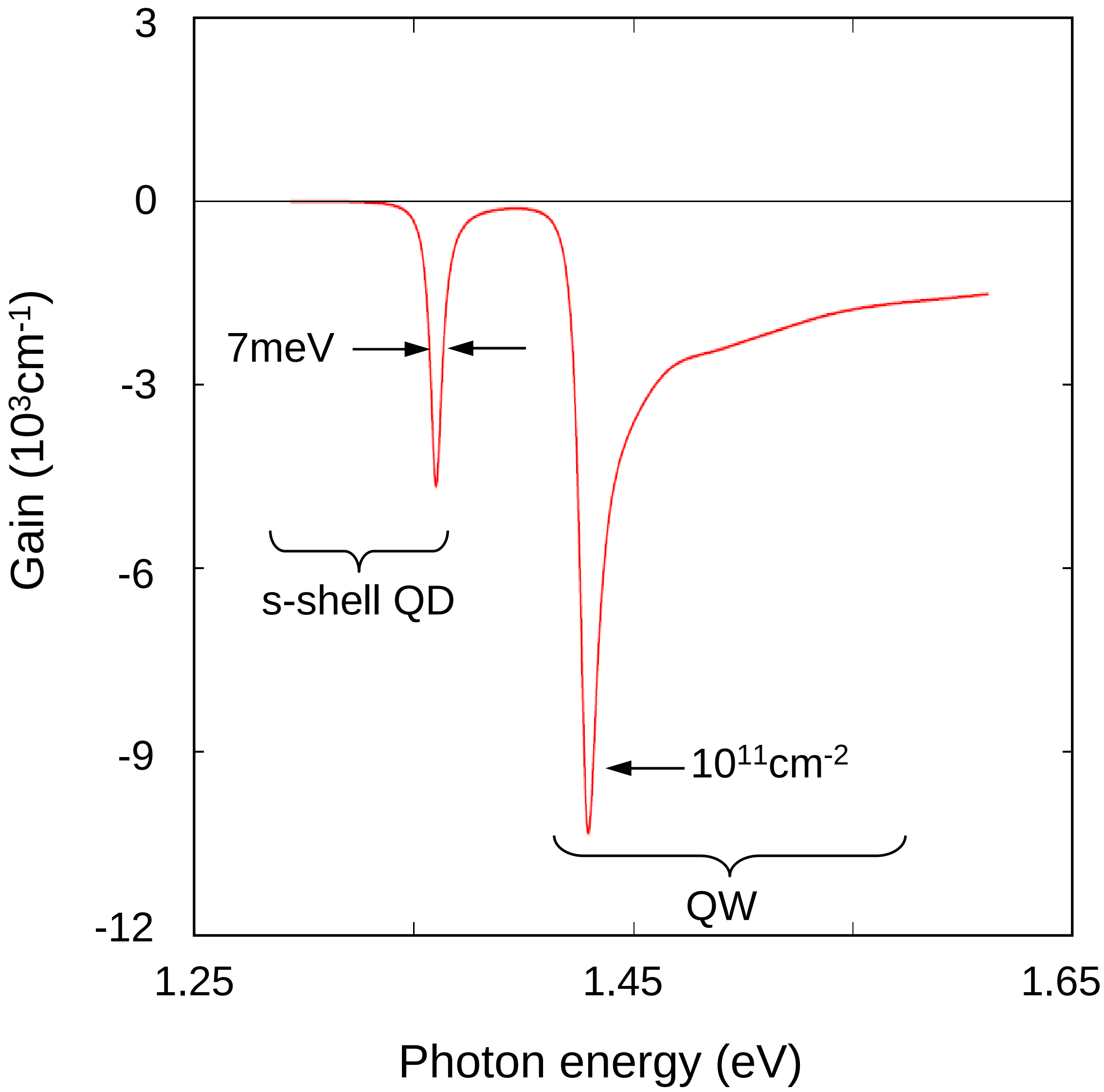

Homogeneously (intrinsically) broadened quantum-dot absorption and gain

InGaAs QD, N_D=5x10^{10}cm^{-2}, T=300K

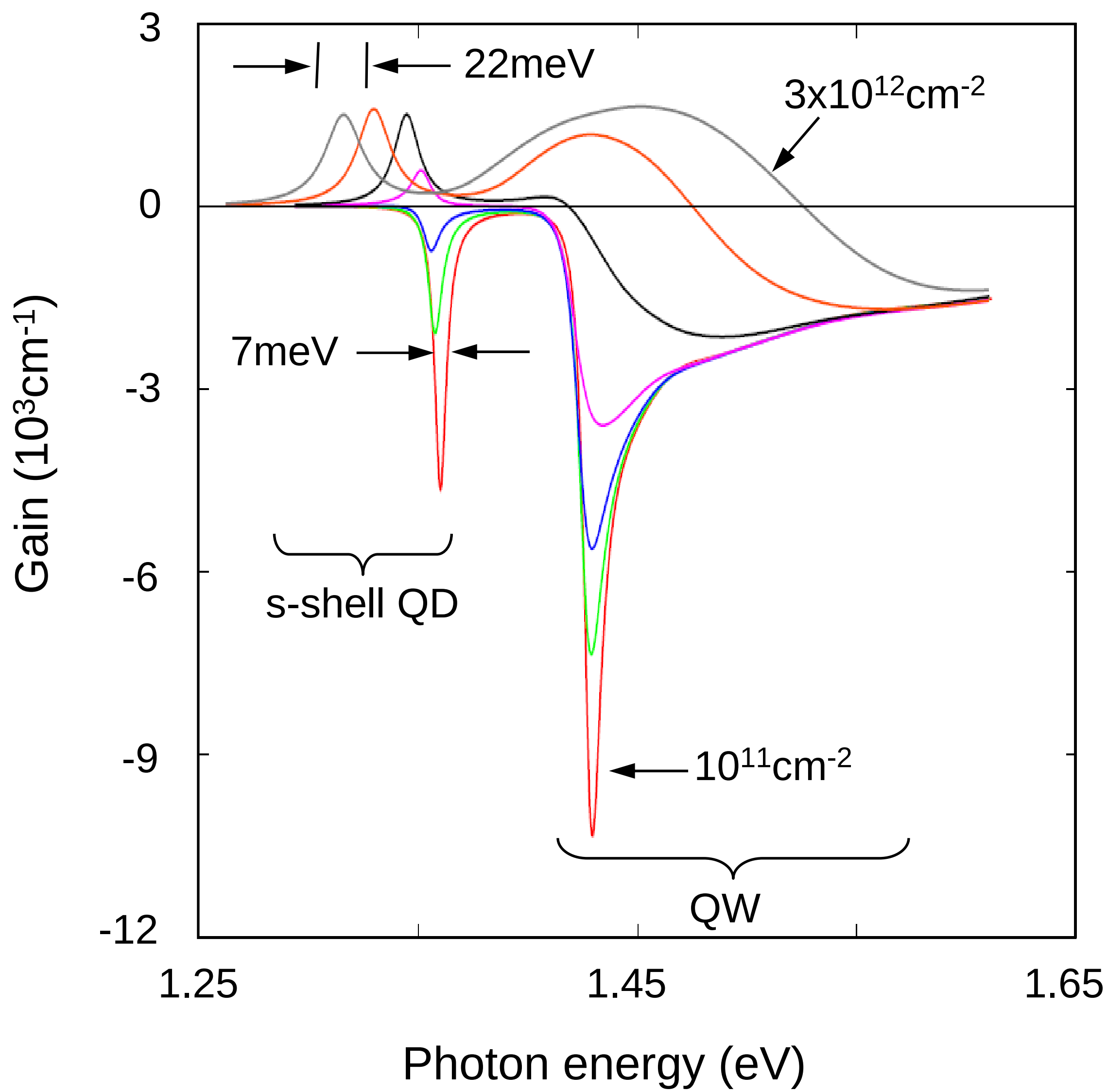

Quantum-dot gain saturation

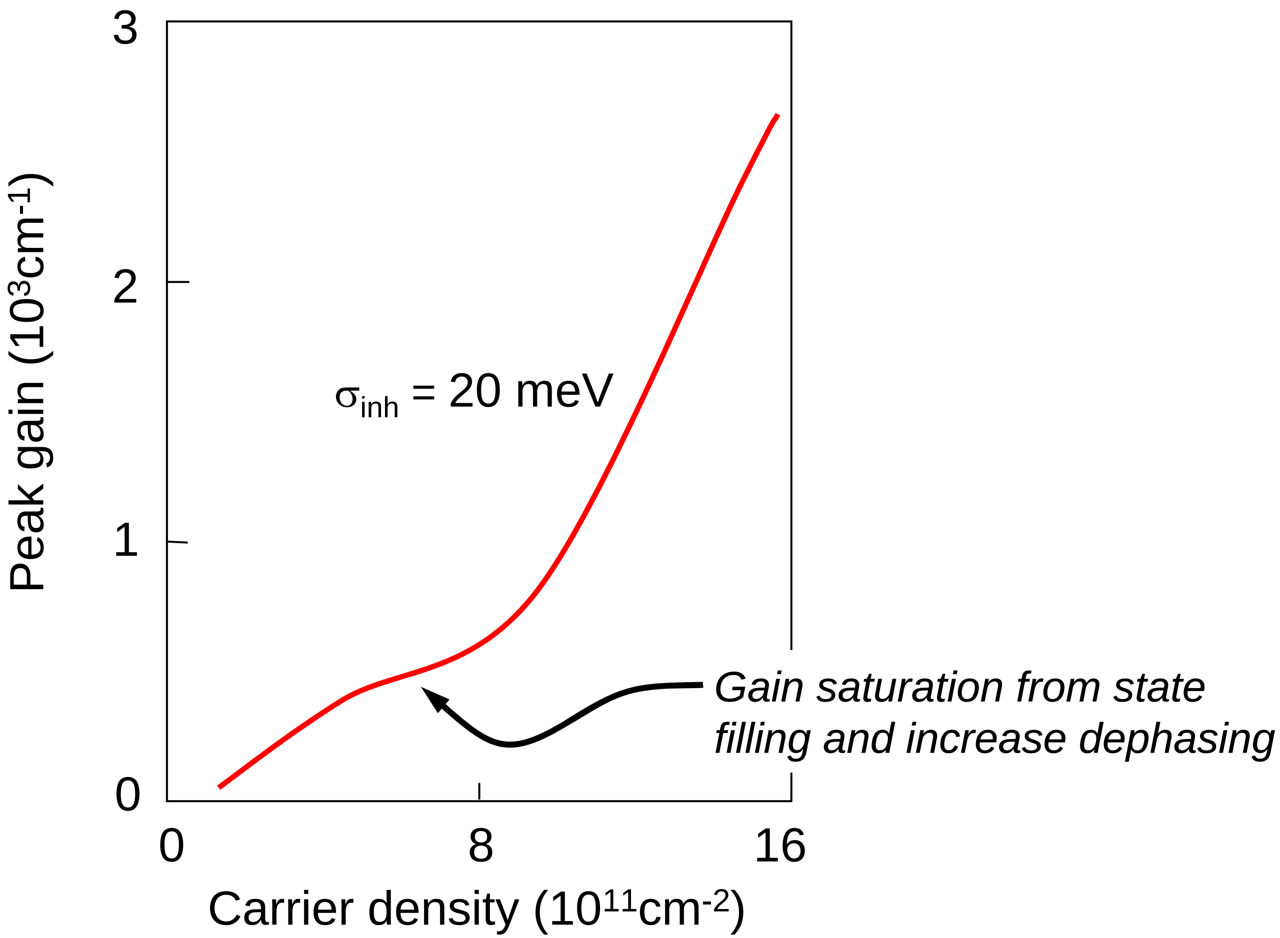

Lorke, WWC, Nielsen, Seebeck, Gartner and Jahnke, PRB **74**, 035334 (2006)

Lorke, Jahnke, WWC, APL **90**, 051112 (2007)

Quantum-dot gain saturation

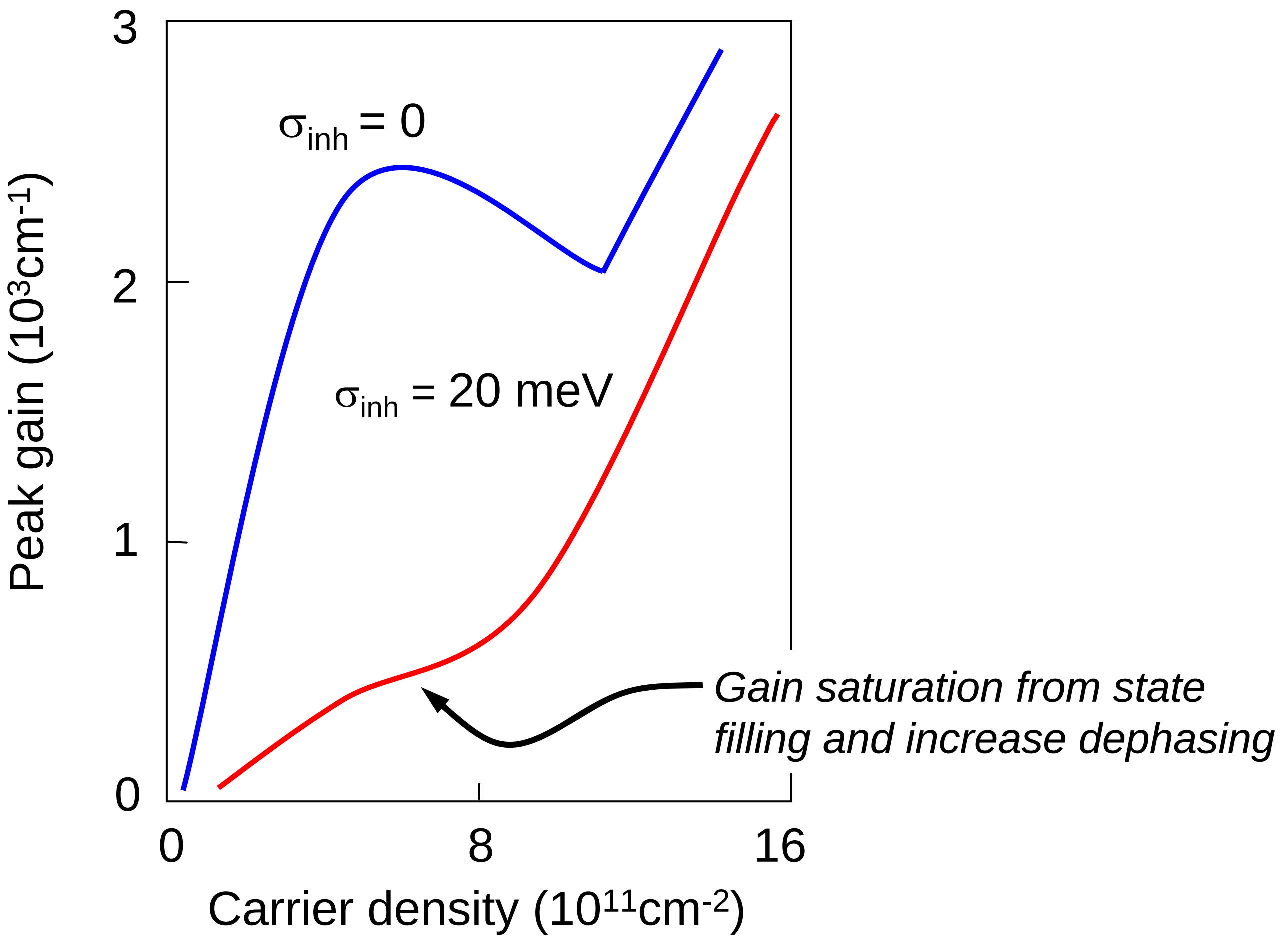

Lorke, WWC, Nielsen, Seebeck, Gartner and Jahnke, PRB **74**, 035334 (2006)

Lorke, Jahnke, WWC, APL **90**, 051112 (2007)

Homogeneously (intrinsically) broadened quantum-dot absorption and gain

InGaAs QD, N_D=5x10^{10}cm^{-2}, T=300K

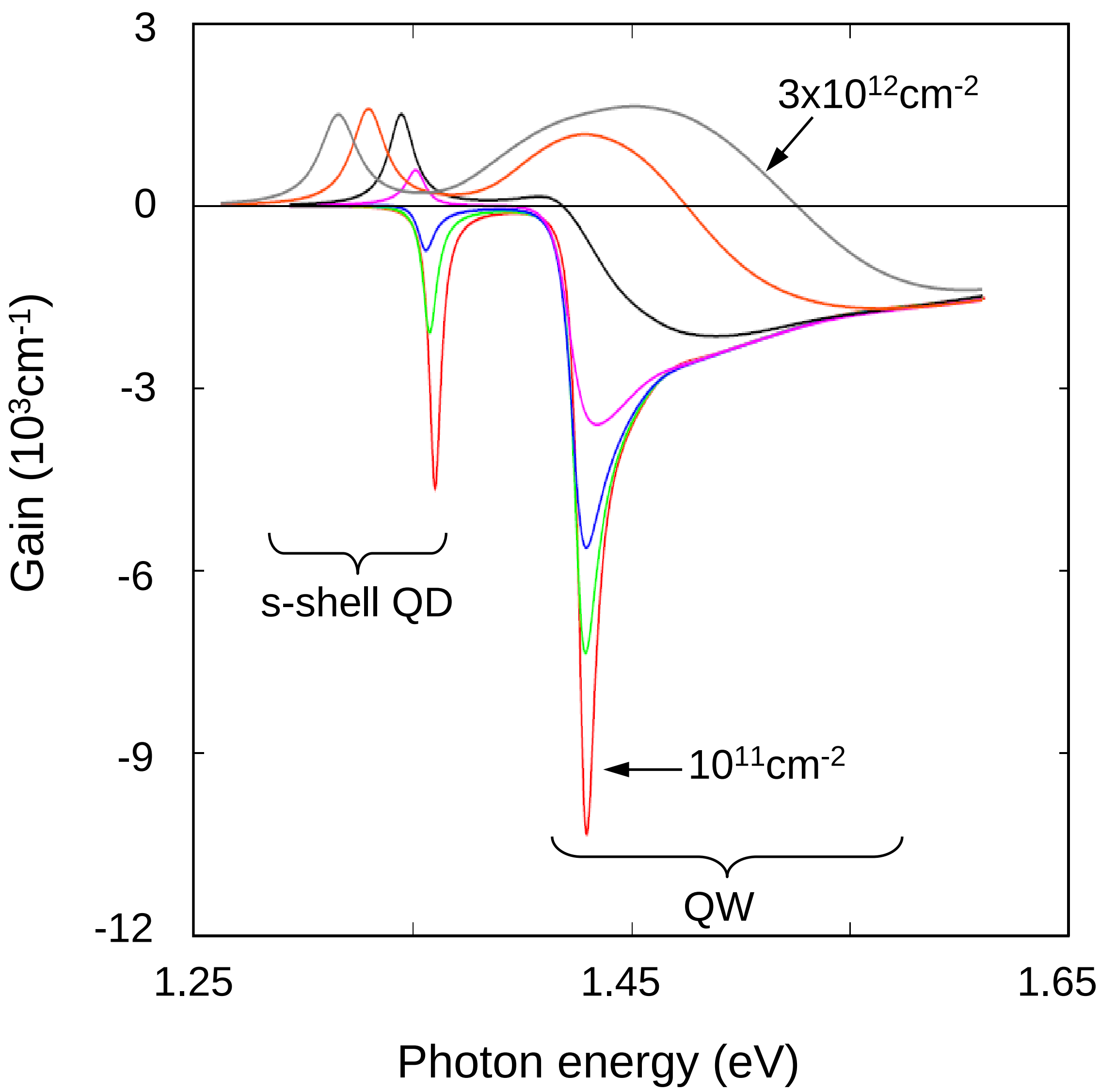

Linewidth enhancement (antiguiding) factor in quantum dots

Many-body calculation

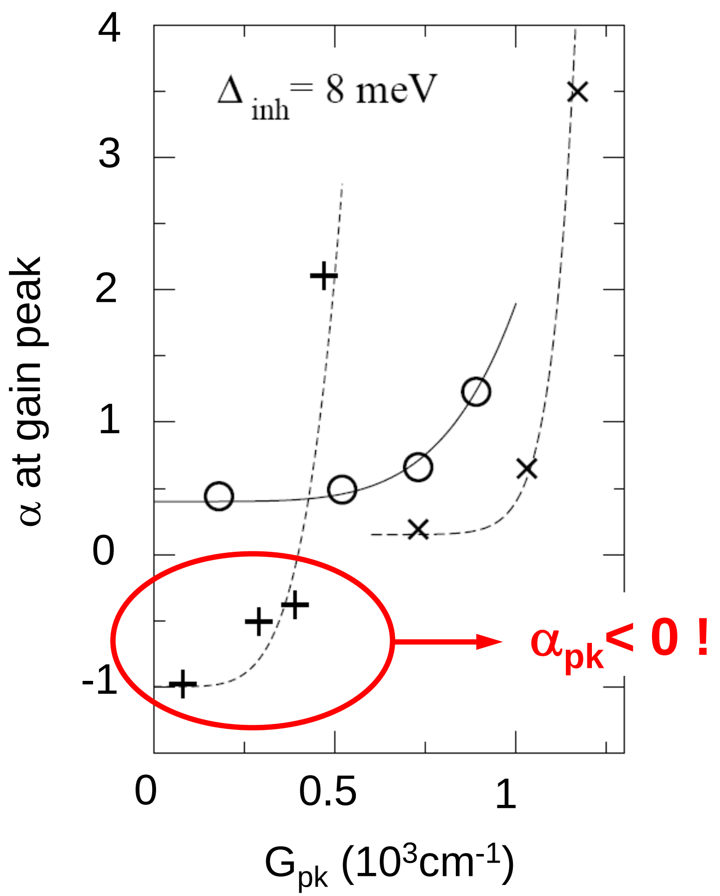

Near field measurements

P. M. Smowton, et al, APL 81, 3251, 2002

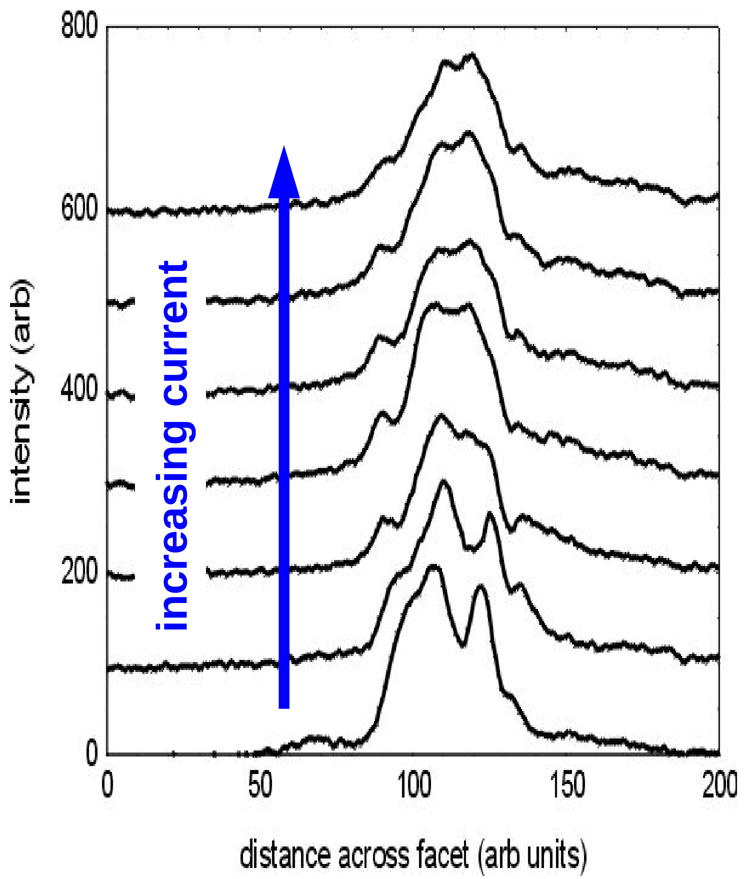

Lorke, Jahnke, WWC, APL **90**, 051112 (2007)

Schneider, WWC, Koch, PRB **66**, Rapid Commun. 41310, 2002

Microscopic theory in laser modeling

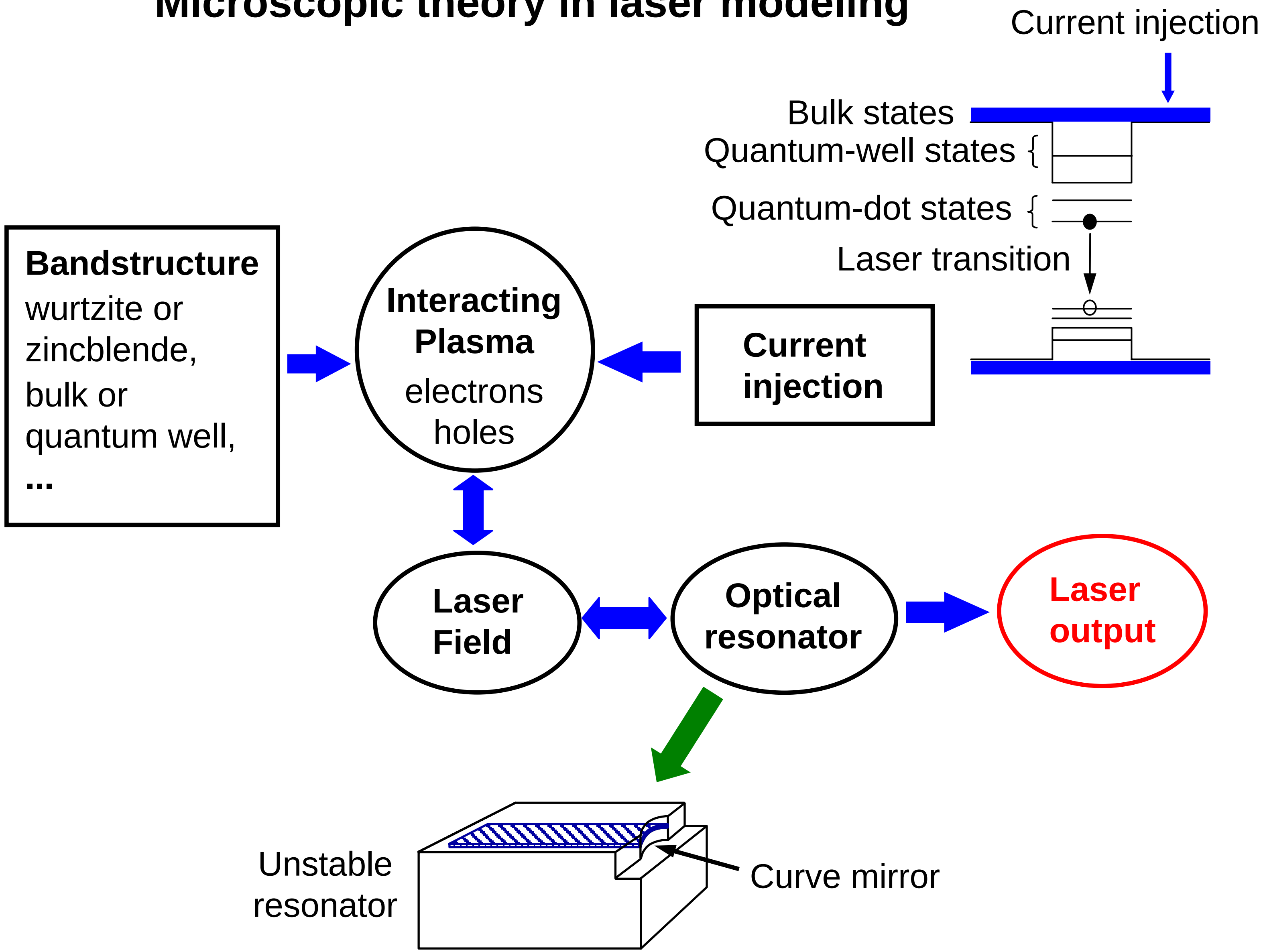

Nonequilibrium dynamics in a quantum-dot laser

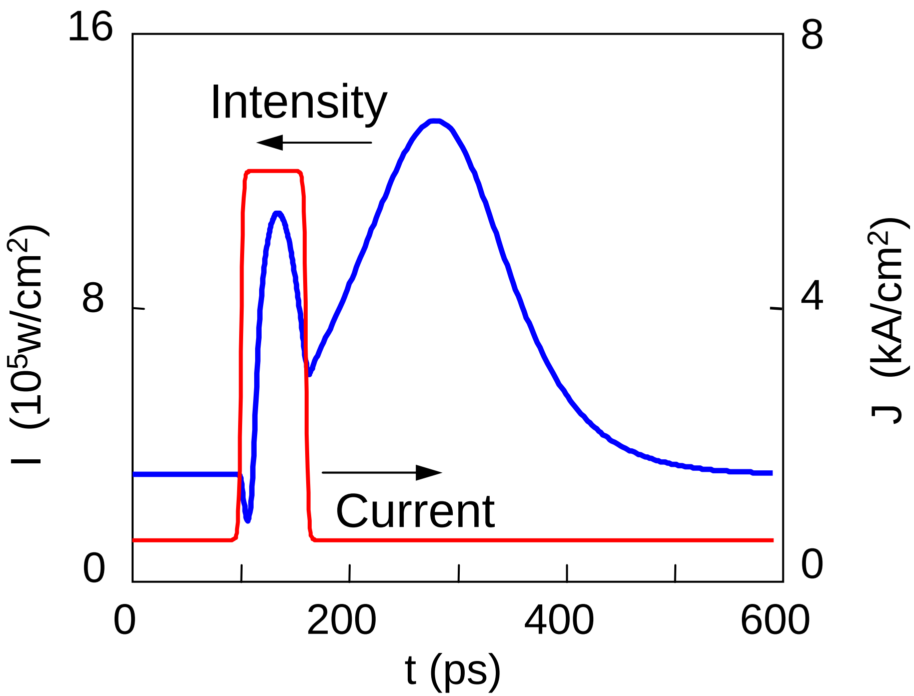

WWC and S. W. Koch, IEEE Journ. Quantum Electron. **41**, 495 (2005)

Nonequilibrium dynamics in a quantum-dot laser

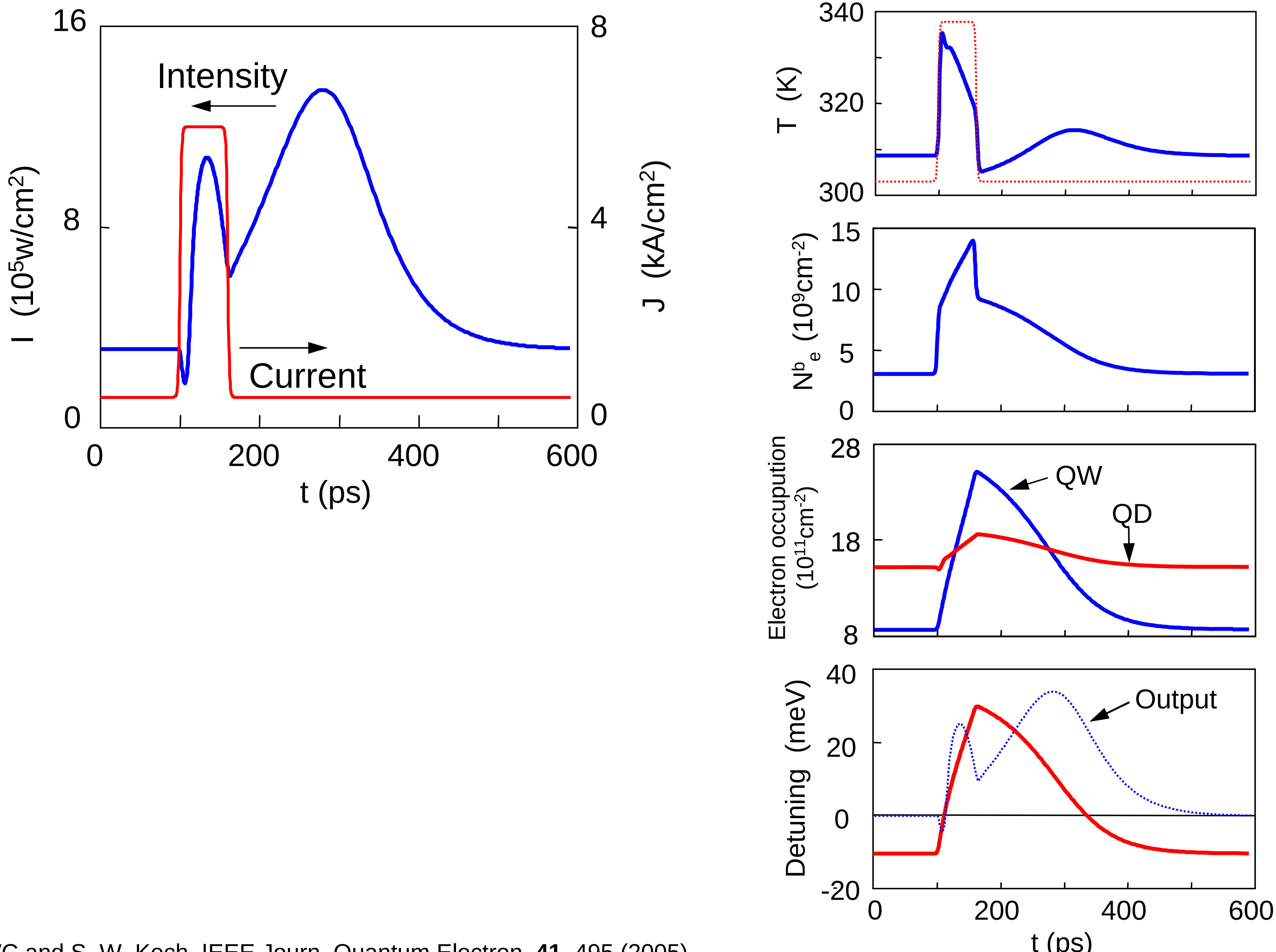

WWC and S. W. Koch, IEEE Journ. Quantum Electron. **41**, 495 (2005)

Nonequilibrium dynamics in a quantum-dot laser

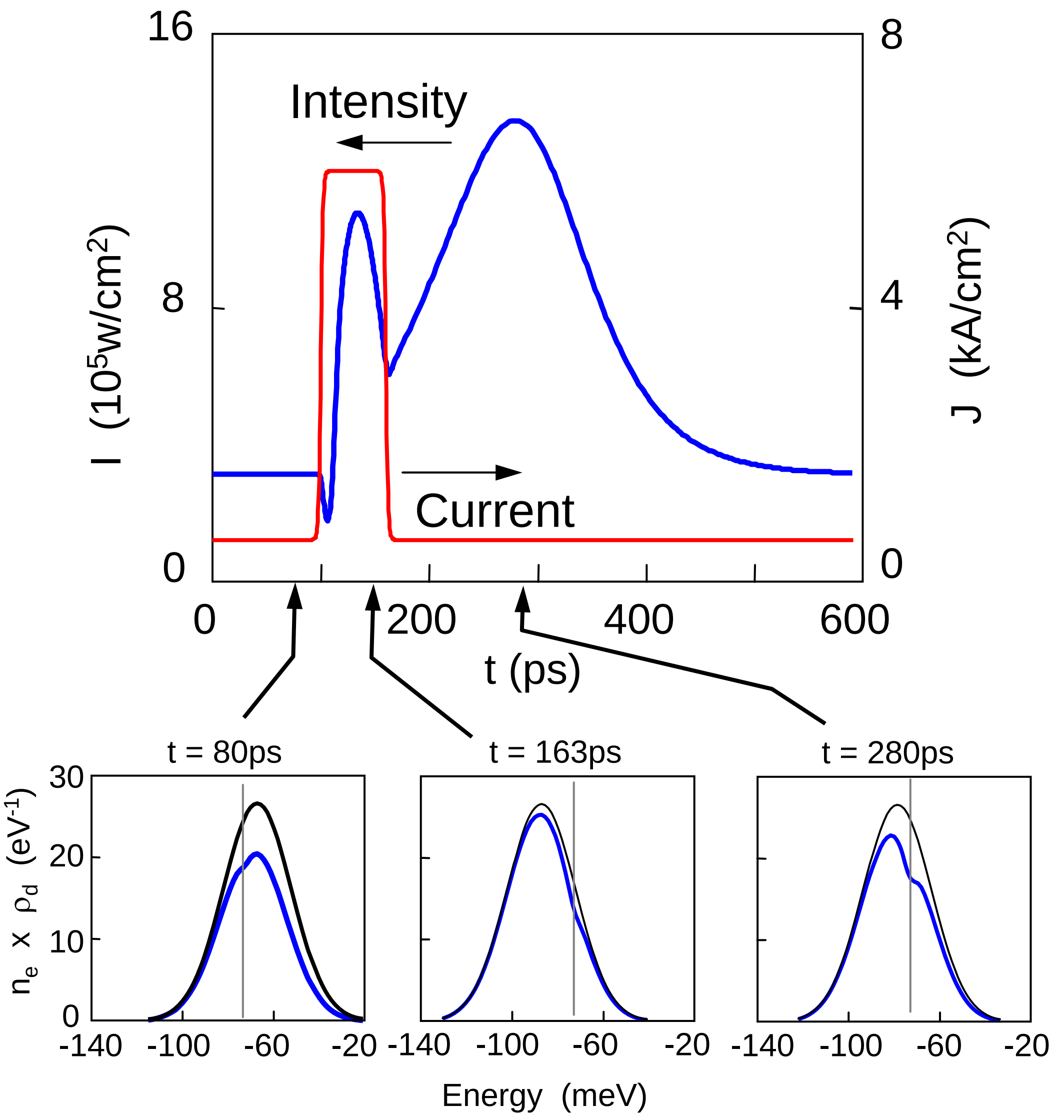

Hole burning in inhomogeneously-broadened quantum-dot population

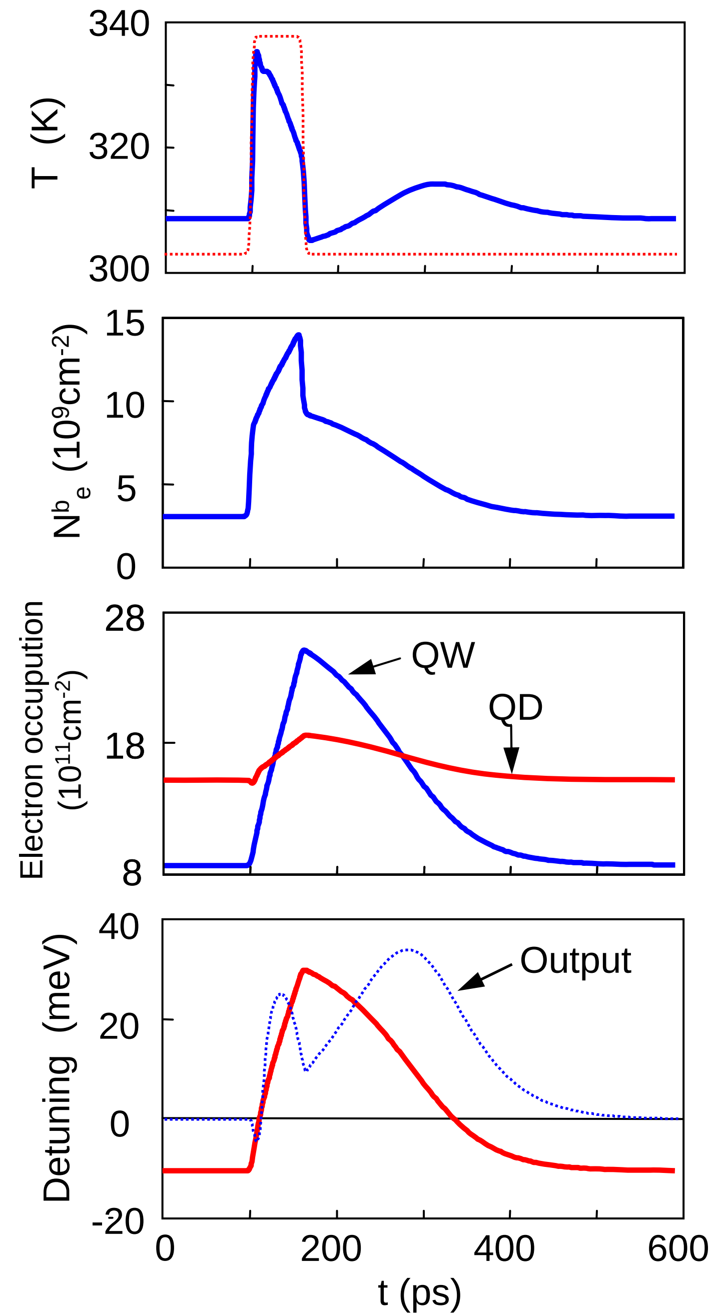

WWC and S. W. Koch, IEEE Journ. Quantum Electron. **41**, 495 (2005)

Summary

1) Past: Free-carrier theory
2) Present: Many-body description
3) Evolving: Quantum-dot gain theory

- Many-body effects $\longleftrightarrow$ Coulomb interaction
- Clean and understandable formulation
- Influences all semiconductor gain properties

Schematic outline of gain approaches

Many body

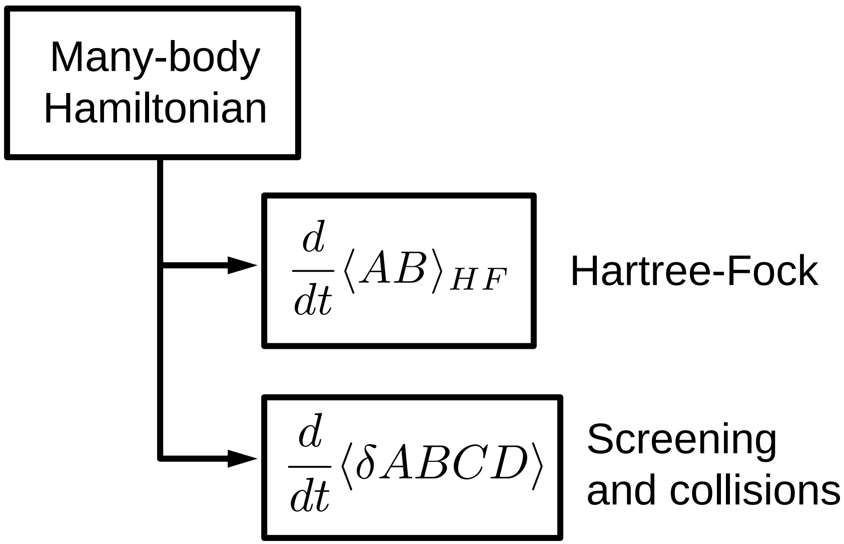

Free carrier

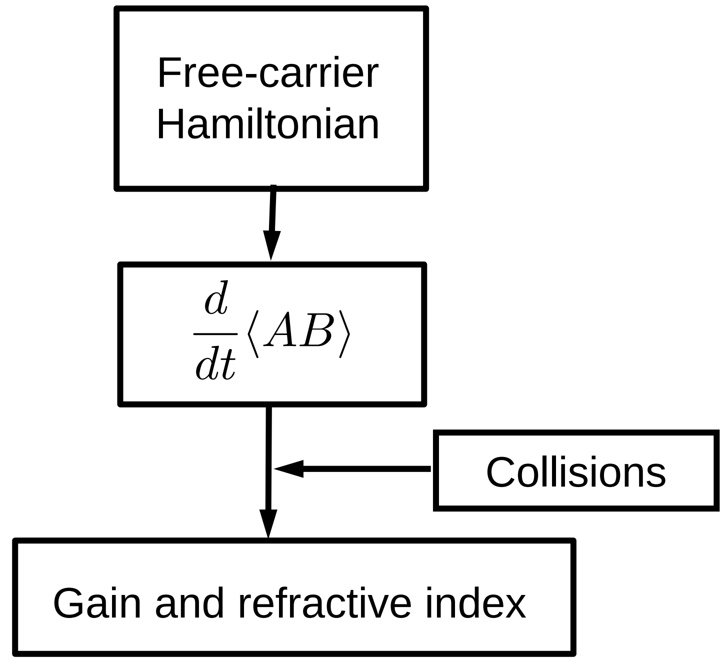

Summary

1) Past: Free-carrier theory
2) Present: Many-body description
3) Evolving: Quantum-dot gain theory

- Many-body effects ⟷ Coulomb interaction
- Clean and understandable formulation
- Influences all semiconductor gain properties

<u>Free-carrier calculation</u> → <u>Many-body calculation</u>

Accounts for collisions (a many-body effect)

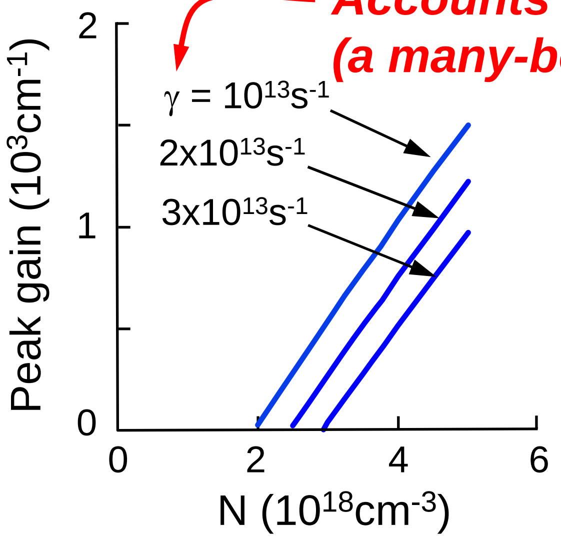

Peak gain sensitive to free parameter γ

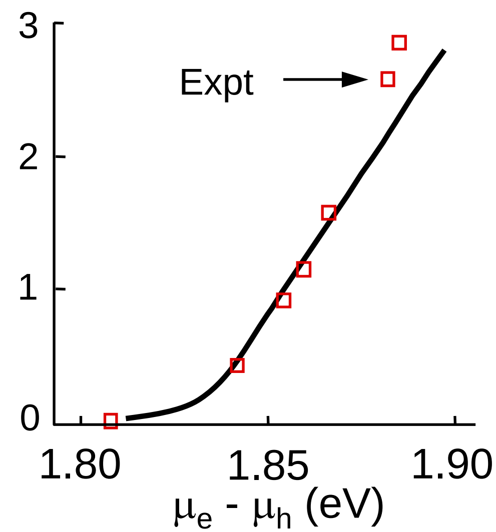

Gain peak properties precisely and accurately determined

Uses of gain theory

Bandstructure
wurtzite or zincblende, bulk or quantum well, ...

Interacting Plasma
electrons
holes

Laser Field

Gain and refractive index

+

Extrinsic properties
inhomogeneous broadening, carrier leakage and capture, nonradiative losses, ...

Expts

Extraction of extrinsic properties

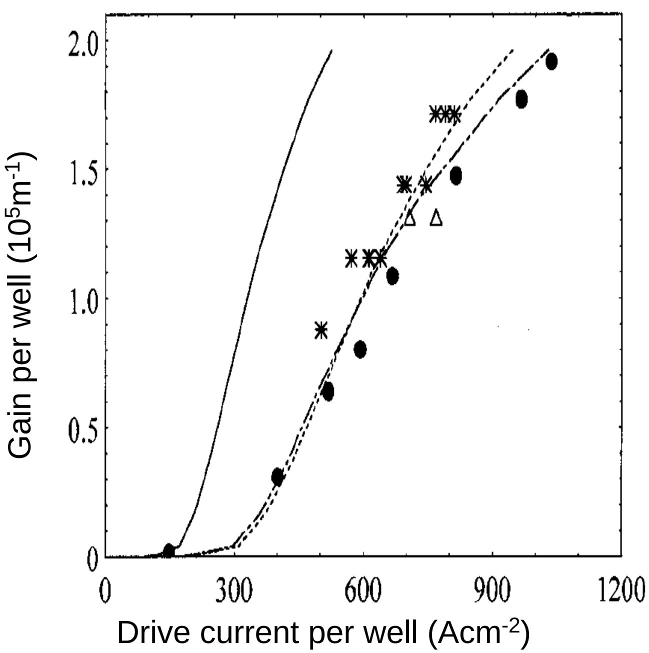

P.M. Smowton, P. Blood (Cardiff) and WWC APL 76, 12 (2000)

Wide bandgap Group-III Nitrides: very strong many-body effects

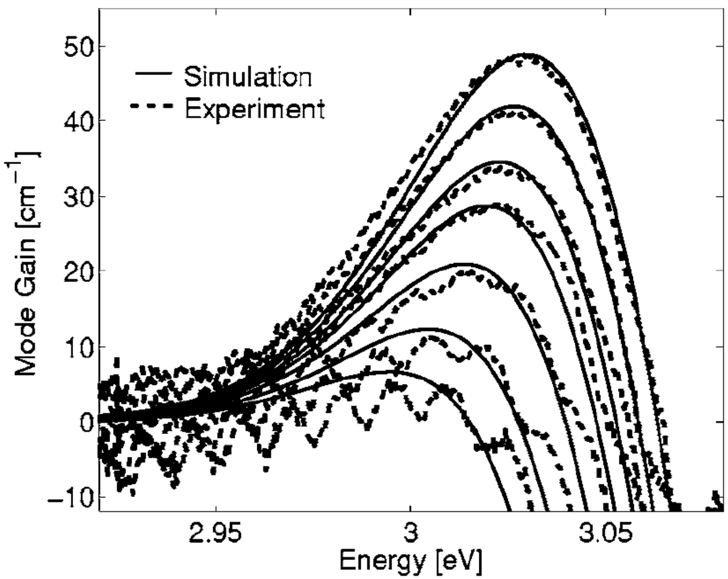

B. Witzigmann (ETH Zürich), et al, APL **88**, 021104 (2006)

U.T. Schwarz (Univ. Regensburg), et al, APL 83, 4095 (2003)

α at gain peak

Expt.

Theory

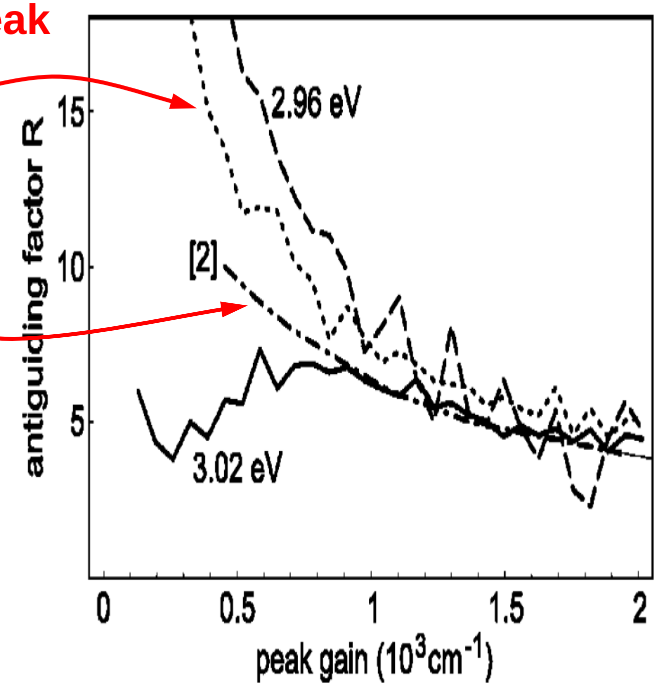

FIG. 4. Antiguiding factor R as function of peak gain at $E=3.02$ eV (solid curve), $E=2.96$ eV (dashed curve), and at the energy of the carrier-density-dependent peak gain (dotted curve). For comparison results from simulations for a single 2 nm QW is given (dot–dashed curve, from Ref. 2).

$$g + iK_0\delta n = i\frac{\omega}{\varepsilon_0 ncE}P$$

$$\alpha = R = -\frac{d\left(\delta n\right)/dN}{dg/dN}$$

Antiguiding factor

α factor

W.W.C, H. Amano and I. Akasaki, APL 76, 1647 (2000)

Polarization equation of motion

$$\omega_k^{(0)} - \sum_{\mathbf{k}'} V_{kk'} \left(n_{ek'} + n_{hk'}\right)$$

$$\frac{2\mu_k E}{\hbar} + \sum_{k'} V_{kk'} p_{k'}$$

$$\frac{dp_k}{dt} = -i\omega_k p_k - i\Omega_k \left(n_{ek} + n_{hk} - 1\right)$$

$$+ S_k^{c-c} + S_k^{c-p}$$

$$-\sigma_k^d p_k + \sum_k \sigma_{k,k'}^{nd} p_{k'}$$

Diagonal **Nondiagonal**

$$-p_\alpha \frac{2}{\hbar} \sum_{\mathbf{k}'} \sum_{\mathbf{q}} \sum_{\sigma} \sum_{\sigma'} \sum_{\mathbf{k}} \xi_{\alpha k} \left[{W_q}^2 - \frac{\delta_{\sigma,\sigma'}}{2} W_q W_{|\mathbf{k}'-\mathbf{q}-\mathbf{k}|} \right] \frac{1}{\Delta - i\delta\varepsilon}$$
$$\times \left[n_{|\mathbf{k}'-\mathbf{q}|\sigma'} \left(1 - n_{k'\sigma'}\right)\left(1 - n_{k\sigma}\right) + \left(1 - n_{|\mathbf{k}'-\mathbf{q}|\sigma'}\right) n_{k'\sigma'} n_{k\sigma} \right]$$

Typical

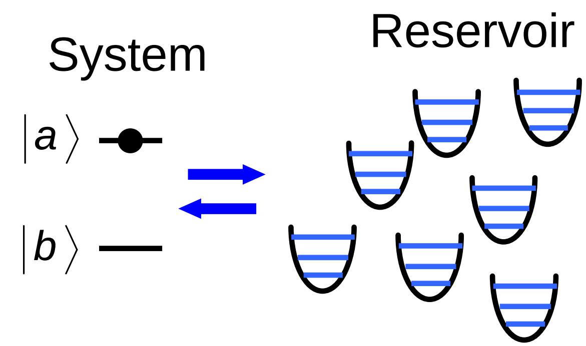

Semiconductor

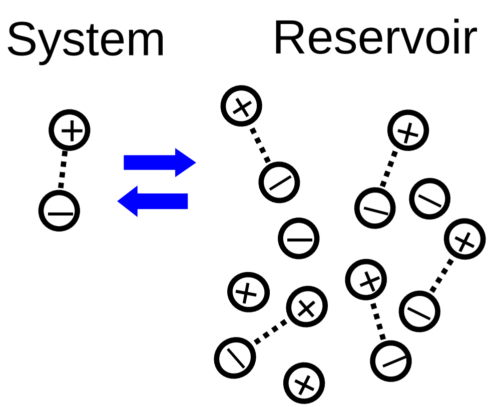

System is its own reservoir

Barrier Influence on Threshold Current Density in AlGaN Lasers

Chow (Sandia), Kneissl (Technical U, Berlin), Johnson and Northrup (PARC)

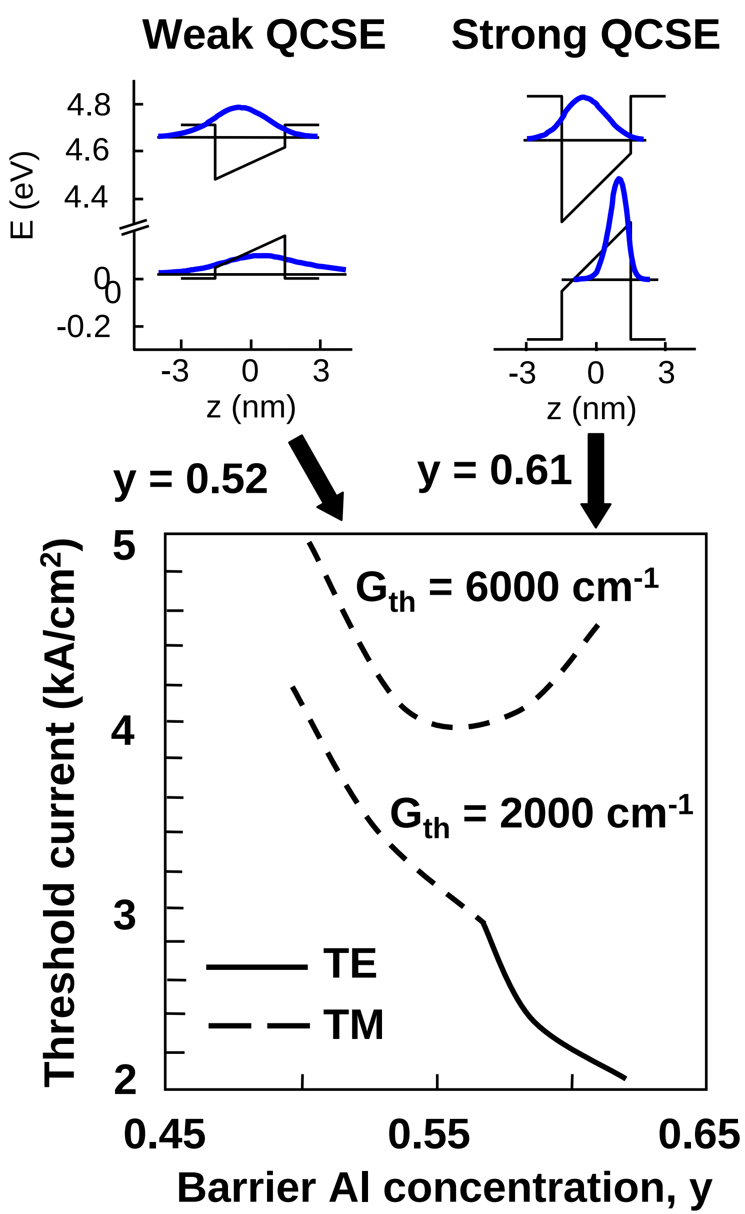

Simulation Model

- 3nm $Al_{0.46}Ga_{0.54}N$ / $Al_yGa_{1-y}N$, 300K, 280 nm
- Many-body gain theory with carrier-carrier scattering treated at level of quantum kinetic theory (no T_2 free parameter)
- Band structure calculated with 6x6 **k·p** theory and Poisson equation
- Threshold current contributions: spontaneous emission, non-radiative losses and carrier leakage

Highlights

- Significant variation in threshold properties with barrier composition and threshold gain
- Gain structure optimization possible by changing only barrier configuration (and, hence, preserving emission wavelength)
- Predictive theory with only gain structure and bulk material parameters as input can facilitate laser design optimization

W.W. Chow, M. Kneissl, J.E. Northrup and N.M. Johnson, APL **90**, 101116 (2007)

Computational Simulation of UV Nitride Laser Heterostructures (supporting information for simulation slide)

The graph in the lower left-hand quadrant illustrates the sensitivity of laser threshold current density to Al concentration, y, in an $Al_{0.46}Ga_{0.54}N$ quantum well structure with $Al_yGa_{1-y}N$ barrier regions. The quantum well composition is chosen to give an emission wavelength of approximately 280 nm, which is useful for excitation of important biomolecules. The results suggest that optimization of laser gain configuration is possible by varying the barrier composition, with the quantum well width and composition remaining unchanged, thus preserving other desired laser properties such as the emission wavelength. The appreciable changes in threshold properties arise from changes in the quantum confinement Stark effect as illustrated in the top left-hand diagrams. The complicated behavior depicted in this slide is describable by a many-body theory that can be used to facilitate laser gain structure optimization for deep UV nitride laser heterostructures. Coordinating such computational optimization with growth of MQW heterostrutures will accelerate progress toward the realization of deep UV laser diodes.